7
Uroradiology

Standard Protocols for the Urinary Tract

Kidneys

Renal tumors are often identified on ultrasound examinations or on CT examinations incidentally. Dynamic CT using MDCT enables to characterize and stage the renal lesions, and to provide the anatomical information for blood vessels, and urinary systems in a single examination. In addition, it is used to evaluate lymph node and distant metastasis.

If contrast-enhanced CT is contraindicated such as due to iodine allergy, the primary lesion is diagnosed by MRI. Bone scintigraphy is performed if bone metastasis is suspected. PET might be useful for evaluating recurrence.

In dynamic contrast-enhanced study with either CT or MRI, the following four phases are observed following rapid contrast medium injection (3 to 5 mL/s).

① Arterial phase

This is the period from approximately 20 to 30 s after the start of contrast medium administration, when the renal artery is strongly enhanced. It is useful for evaluating 3D arterial images.

② Corticomedullary phase

This is the period from 30 to 70 s after the start of contrast medium administration, when mainly the renal cortex is enhanced. Imaging in the early corticomedullary phase (30 to 40 s) enables the renal arteries and veins to be assessed. This phase is advantageous when evaluation of the arteries and veins is required or when tumor vascularity is evaluated.

③ Nephrographic phase

This is the period from 80 to 130 s after the start of contrast medium administration, when the renal cortex and medulla are comparably enhanced and the renal parenchyma shows uniform attenuation. This is the best phase for lesion detection and staging.

④ Excretory phase

This is the period beginning 180 s after the start of contrast medium administration, during which the contrast medium is excreted and the urinary tract is visualized. This phase is suitable for evaluating tumor invasion into the renal pelvis.

In clinical practice, the phases required to meet the objectives of the examination are selected from among the 4 described above.

1. When a tumorous lesion is suspected

① CT

The following phases are usually acquired when a renal tumor is suspected.[1)]

(1) Non-contrast

(2) Corticomedullary phase (~ 30 to 40 s after the start of contrast medium administration, Fig. 1A)

(3) Nephrographic phase (~ 100 s after the start of contrast medium administration)

(4) Excretory phase (~ 180 s after the start of contrast medium administration)

Both characterization and staging can be accomplished. Non-contrast CT is important for differentiating benign tumors, i.e. diagnosing angiomyolipomas.

Approximately 100 mL of a non-ionic contrast medium is administered in 30 s. An injection rate of ≥ 3 mL/s is suitable for obtaining good arterial images. Because the contrast arrival time to the aorta varies in individuals, bolus tracking should be used.

The scanning range should completely cover the both kidneys. When chest imaging is used for screening pulmonary metastasis, good enhancement of the blood vessels in the chest is maintained in the nephrographic phase, which facilitates the evaluation of lymph nodes that attach to the blood vessels. However, the imaging can be performed in any phase.

In general, a 5-mm-slice thickness is applied. For small lesions, thinner slice reconstruction, of approximately 3-mm thickness, would be applied. Thin-slice images are required to obtain MPR images such as coronal and sagittal plane images. When evaluating the vascular anatomy preoperatively, 3D CTA images should be generated using a slice thickness of approximately 1 mm.

Non-contrast CT and nephrographic phase CT alone are sufficient for follow-up (including the chest).

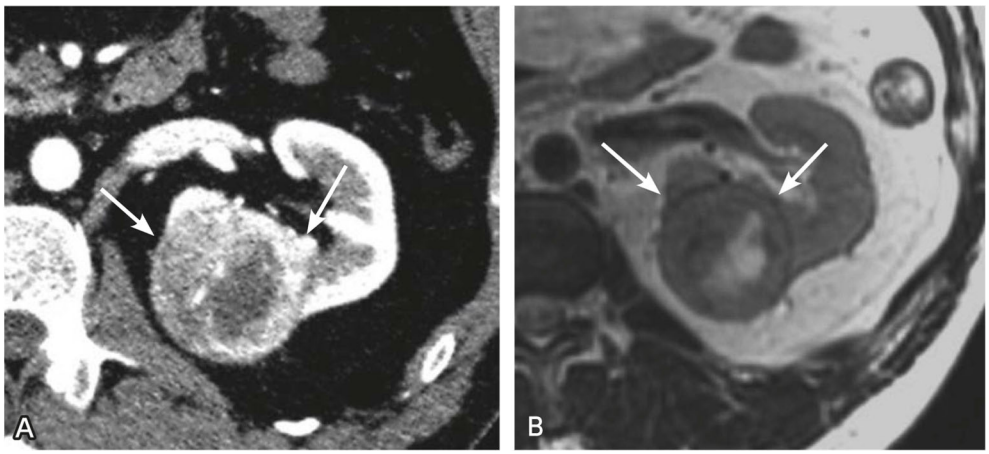

Figure 1. Left renal cell carcinoma (RCC)

A: Dynamic CT, corticomedullary phase, 35 s after contrast medium administration: Inhomogeneous strong enhancement (→) indicated abundant tumor blood flow.

B: MRI, T2-weighted transverse image: a pseudocapsule is seen around the tumor (→).

Table 1. Examples of RCC sequences (phased-array coil)

Imaging Method	Sequence	1.5T		3T		Other
		TE/TR	Slice thickness	TE/TR	Slice thickness	
(1) T2-weighted imaging/transverse, coronal	Breath-hold FSE	Approx. 3000/100 ms (ETL approx. 12)	4 to 8 mm	Approx. 3000/90 ms (ETL approx. 20 to 24)	3 to 8 mm	
	Respiratory-gated FSE	R-R interval /approx. 90 ms	4 to 8 mm	R-R interval /approx. 90 ms	3 to 8 mm	
	Breath-hold heavy T2-weighted	∞ /approx. 80 ms	4 to 8 mm	∞ /approx. 80 ms	3 to 8 mm	
(2) Pre-contrast T1-weighted imaging	3D GRE	4 to 5 /approx. 1.2 to 2 ms	4 to 8 mm	4 to 5 /approx. 1.2 to 2 ms	3 to 8 mm	Imaging times: 30, 60 to 90, and 150 to 180 s after injection
(3) Dynamic MRI	3D GRE	4 to 5 /approx. 1.2 to 2 ms (FA approx. 12 to 15°)	4 to 8 mm	4 to 5 /approx. 1.2 to 2 ms (FA approx. 12 to 15°)	3 to 8 mm	
(4) Diffusion-weighted imaging	Respiratory-gated 2D-EPI	R-R interval /approx. 100 ms	4 to 8 mm	R-R interval /approx. 100 ms	3 to 8 mm	b-value = 0, 750 to 1,000 s/mm^2

② MRI

The following types of imaging are usually used when performing an MRI evaluation.[2)]

(1) T2-weighted imaging (transverse and coronal)

(2) Pre-contrast T1-weighted imaging

(3) Dynamic MRI using a contrast medium

(4) Diffusion-weighted imaging

Both characterization and staging can be performed with this protocol.

The imaging range sufficiently covers both kidneys. The slice thickness is approximately 3 to 8 mm. The recommended parameters are shown in Table 1. As in-phase and opposed-phase imaging enables detection of a mixture of water and fat, tumors with intracellular lipid, such as clear cell carcinomas, can be diagnosed. T2-weighted imaging is useful for detecting pseudocapsules in renal cell carcinoma (Fig. 1B). In addition, several reports show that diffusion-weighted imaging is useful for differentiating benign from and malignant lesions, and for determining the aggressiveness of cancer.[3)]

2. When an infectious lesion is suspected

Since CT is standard modality of choice, MRI is rarely applied. The following phases of CT imaging are usually performed.

① Non-contrast

② Post-contrast imaging (70 to 90 s after the start of contrast medium administration)

The contrast injection rate should be ≥ 2 mL/s. The imaging range sufficiently covers the kidneys. A 5 mm-thick reconstruction is usually applied.

Some literature recommends post-contrast tri-phasic dynamic study as shown below.[4)]

① Non-contrast

② Corticomedullary phase (30 s after the start of contrast medium administration)

③ Nephrographic phase (70 to 90 s after the start of contrast medium administration)

④ Excretory phase (5 min after the start of contrast medium administration)

However, the nephrographic phase is considered superior to the corticomedullary and excretory phases for detecting lesions and evaluating its spread.[5] In view of the radiation exposure, pre-contrast and tri-phasic post-contrast studies are hardly implemented. It is appropriate to perform pre-contrast and the nephrographic phase CT, adding excretory-phase imaging only if urinary tract obstruction is suspected.[5]

Imaging methods for the upper urinary tract

In the evaluation of the upper urinary tract, CT is the modality of choice for lesion detection, determining invasion depth, and screening for lymph node and distant metastases. MDCT (≥ 16-row CT) enables this information to be obtained with a single examination. CT urography, pre- and post-contrast excretory-phase imaging with thin slice, is widely used to evaluate the urinary tract.[6, 7] MRI may be used in cases where a contrast medium is contraindicated, such as in cases with iodine allergy.

1. When urolithiasis is suspected

When painful hematuria is present, and imaging is performed to detect urinary stones, non-contrast CT imaging is performed from the upper pole of the kidney to the pelvic floor using a slice thickness of 3 to 5 mm and pitch of 1 to 1.5.

Low-dose imaging provides sufficient diagnostic performance for detecting urinary stones. Consequently, imaging that reduces radiation exposure as much as possible is performed.

2. When a tumor is suspected

① CT

The following imaging (CT urography protocol) is performed, when screening for upper urinary tract tumor; such as when there is painless hematuria (in elderly persons), past history of urothelial neoplasia, or bladder cancer.[6, 7]

(1) Non-contrast CT

(2) Nephrographic phase (~ 100 s after the start of contrast medium administration)

(3) Excretory phase (~ 8 min after the start of contrast medium administration, Fig. 2)

Similar to the urolithiasis protocol, non-contrast CT imaging is performed first and covers the area from the upper pole of the kidney to the inferior margin of the pubic bone. A contrast medium is then administered. Because visualization of the urinary tract in the excretory phase tends to be dose-dependent, a dose of approximately 600 mgI/mL/kg BW (body weight (kg) × 2 mL for 300 mgI/mL agent) is recommended. The contrast medium is administered in approximately 30 s, and the entire kidneys are scanned approximately 100 s after the start of contrast injection (nephrographic phase). Approximately 8 to

10 min after the start of contrast medium administration, excretory phase images are acquired from the upper pole of the kidney to the inferior margin of the pubic bone. In cases of screening for metastasis in the chest, the nephrographic phase image is suitable for evaluating the hilar lymph nodes. However, any phase is acceptable for evaluating the lung. Urinary bladder tumors can be visualized as filling defects by having the patient urinate once after nephrographic phase imaging, waiting approximately 40 min, and then performing excretory phase imaging approximately 45 min after urination. This enables excretory-phase imaging to be performed with the whole urinary bladder filled with homogeneous contrast medium.[7)]

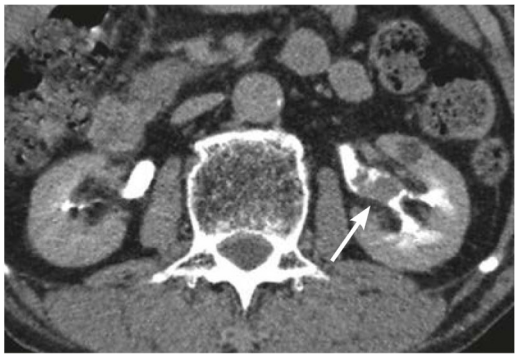

Figure 2. Left renal pelvic cancer

Dynamic CT, excretory phase, 8 min after contrast medium administration: A tumor is seen in the left renal pelvis (→).

Table 2. Examples of ureteral cancer sequences (phased-array coil)

Imaging Method	Sequence	1.5T		3T		Other
		TE/TR	Slice thickness	TE/TR	Slice thickness	
(1) T2-weighted/transverse and coronal	Breath-hold FSE	Approx. 3,000/90 ms (ETL approx. 15)	4 to 8 mm	Approx. 3,000/90 ms (ETL approx. 20 to 24)	3 to 8 mm	
	Respiratory-gated FSE	R-R interval/approx. 90 ms	4 to 8 mm	R-R interval/approx. 90 ms	3 to 8 mm	
	Breath-hold heavy T2-weighted	Infinite/approx. 80 ms	4 to 8 mm	Infinite/approx. 80 ms	3 to 8 mm	
(2) Pre-contrast T1-weighted	3D GRE	4 to 5/approx. 1.2 to 2 ms	4 to 8 mm	4 to 5/approx. 1.2 to 2 ms	3 to 8 mm	
(3) Post-contrast, fat-suppressed, T1-weighted/transverse and coronal	3D GRE	4 to 5/approx. 1.2 to 2 ms (FA approx. 12 to 15°)	4 to 8 mm	4 to 5/approx. 1.2 to 2 ms (FA approx. 12 to 15°)	3 to 8 mm	
(4) Diffusion-weighted imaging	Respiratory-gated 2D-EPI	R-R interval/100 ms	4 to 8 mm	R-R interval/100 ms	3 to 8 mm	b-value = 0, 750 to 1,000 s/mm^2
(5) MR urography	Projection					
	Fat-suppressed RARE	≥ 4,000/approx. 1,250 ms	4 to 80 mm	≥ 6,000/ approx. 1,200 ms	4 to 80 mm	
	Multislice					
	Fat-suppressed heavy T2-weighted	Infinite/approx. 80 ms	4 to 5 mm	Infinite/approx. 80 ms	4 to 5 mm	
	Respiratory-gated FSE	R-R interval/100 ms		R-R interval/100 ms		

Thin slices provide better performance for detecting small lesions. Reconstruction using a slice thickness of ≤ 3 mm is therefore recommended. MPR images, such as excretory-phase, thin-slice, coronal images, are generated as needed.

To improve urinary tract visualization, oral hydration with water before and after contrast medium administration is desirable.

This imaging method enables both lesion detection and staging to be performed.

② MRI

If upper urinary tract tumor is the main target disease, the following imaging methods are implemented.

(1) T2-weighted imaging (transverse and coronal)
(2) Pre-contrast T1-weighted imaging
(3) Post-contrast, fat-suppressed, T1-weighted imaging (transverse and coronal)
(4) Diffusion-weighted imaging
(5) MR urography

Of these, diffusion-weighted imaging is also highly useful for detecting lesions, distinguishing between benign and malignant lesions, and staging.[8, 9)]

The imaging range for the above is the entire abdomen, including both kidneys, using a slice thickness of approximately 3 to 8 mm. There are two types of MR urography based on the slice thickness used; projection imaging with a single thick-slice slab or, multislice imaging with reconstruction of the multiple slices acquired. The imaging is performed under breath-hold. The parameters recommended for each imaging method are shown in Table 2.

The urinary bladder[10, 11)]

MRI is used for the local staging of bladder cancer. CT is used mainly to evaluate lymph nodes and distant metastases and local recurrence. Although cystoscopy is used to detect bladder cancer, CT urography is also used on the bladder to evaluate the urinary tract as a whole.

1. CT

The following types of CT imaging are selected and combined depending on the purpose of the imaging: non-contrast CT, arterial phase (20 to 30 s after contrast medium administration), corticomedullary phase (30 to 70 s after contrast medium administration), nephrographic phase (80 to 130 s after contrast medium administration), and excretory phase (beginning 8 min after contrast medium administration). For the contrast medium, 100 mL of a nonionized iodinated contrast agent is administered at a rate of 2 to 3 mL/s. If arterial phase vascular images are to be reconstructed, the contrast medium is administered at a rate of approximately 4 mL/s. Non-contrast CT plus contrast-enhanced CT that includes the excretory phase with a thin-slice (1 to 2 mm) is called CT urography.[12)] Commonly used CT urography protocols are single-bolus technique, in which contrast medium is administered once and imaging is performed 3 times (non-contrast

CT, nephrographic phase, and excretory phase), and split-bolus technique, in which contrast medium administration is divided into two times and imaging is performed twice (plain and mixed nephrographic phase/excretory phase).[12] Because imaging is performed once fewer with the split-bolus technique compared with single-bolus, radiation exposure is proportionally reduced with split-bolus imaging. In a mixed nephrographic/excretory phase with split-bolus imaging, the kidneys show equivalent enhancement as the nephrographic phase and the urinary tract is filled with excreted contrast medium as the excretory phase. The single-bolus technique is chosen for high-risk patients with urothelial carcinoma. Contrast enhancement of bladder cancer tumors is the greatest from the late corticomedullary phase to the early nephrographic phase.[13] With thin-slice imaging, almost all bladder cancer larger than 5 mm are detectable.[14] As thin-slice imaging over a relatively extensive range is required, a scanner with ≥ 16 rows is desirable although a 64-row scanner is not necessary.

2. MRI

Imaging is performed in accordance with the Vesical Imaging-Reporting and Data System (VI-RADS), a standardized imaging method[15] (Table 3). However, the imaging parameters shown are strictly examples and can be appropriately adjusted to suit the specifications of a specific MRI system. MRI of the bladder is performed before transurethral resection of a bladder tumor. The expansion and thickness of the bladder wall vary depending on the amount of urine that has accumulated. For high-quality local staging, the bladder wall should be in a moderately expanded state. In many patients, appropriate bladder distension can be obtained by having the patient urinate once 1 hour before the examination, then drink approximately 500 mL of water before the examination, and refrain from urinating until the examination is completed.

The imaging range includes the entire bladder and the prostatic urethra. The basic imaging plane is the transverse plane, with sagittal or coronal plane imaging added. The optimal plane for determining the invasion depth of bladder cancer is theoretically the plane perpendicular to the bladder wall at the tumor base. However, if multiple bladder cancers are present, or if lesions are present along an extensive area of the wall, imaging in the optimal plane for all of the lesions is difficult due to time restrictions. Moreover, image quality is poor with oblique diffusion-weighted imaging. A slice thickness of approximately 3 to 4 mm is appropriate for T2- and diffusion-weighted imaging. Diffusion-weighted imaging is performed using the EPI method with fat suppression. The imaging is performed using b-values of 0 and 1,000 s/mm^2. For contrast-enhanced imaging, dynamic imaging is performed using an injector. The contrast medium dose is 0.1 mmol/kg, injected at a rate of 1.5 to 2.0 mL/s, with a saline chaser. Imaging is performed before contrast medium administration and 5 or 6 times at 30-s intervals beginning from 30 s after contrast medium administration. It is performed as high-speed GRE T1-weighted imaging in 2D or 3D. The preferred plane is the sagittal plane, which can minimize the number of slices. However, if the sagittal plane is parallel to the bladder wall at the base of the lesion to be evaluated (e.g., if the tumor is on the lateral wall), transverse or coronal imaging is performed. Reconstruction can be performed after the examination for any arbitrary plane if volume data are obtained by 3D imaging. Reconstructing T2- and

diffusion-weighted images in the same plane facilitates comparison during interpretation. Although not essential, a magnetic field strength of 3T, as compared with 1.5T, provides a better signal-to-noise ratio and spatial resolution and permits high-speed imaging, enabling images of suitable quality for diagnosis to be obtained.

Table 3. Examples of bladder cancer sequences (phased-array coil)

	T2-Weighted Imaging	Diffusion-Weighted Imaging	Dynamic MRI
1.5T			
TR (ms)	5,000	4,500	3.3
TE (ms)	80	88	1.2
FA (degree)	90	90	
FOV (cm)	23	27	35
Matrix	256 × 189 to 256	128 × 109	256 × 214
Slice thickness (mm)	4	4	1
Slice interval (mm)	0 to 0.4	0 to 0.4	0
	1 to 2	10 to 15	1
b-value (s/mm^2)	—	0, 800 to 1,000	—
3T			
TR (ms)	4,690	2,500 to 5,300	3.8
TE (ms)	119	61	1.2
FA (degree)	90	90	15
FOV (cm)	23	32	27
Matrix	400 × 256 to 320	128 × 128	192 × 192
Slice thickness (mm)	3 to 4	3 to 4	1
Slice interval (mm)	0 to 0.4	0.3 to 0.4	0
	2 to 3	4 to 10	1
b-value (s/mm^2)		0, 800 to 1,000 (up to 2,000)	

Imaging methods for the prostate gland

MRI, which provides excellent tissue contrast, is suitable for local assessment of the prostate gland. MRI has traditionally been used for local staging after malignancy is proved by prostate biopsy. However, it was found that when MRI is performed after prostate biopsy, the intraprostatic signal is altered by hemorrhage due to biopsy, complicating cancer diagnosis. Consequently, MRI is now increasingly performed prior to biopsy to detect clinically significant prostate cancer. However, depending on the prefecture, pre-biopsy MRI may not be approved for medical fee reimbursement. The effect of bleeding can be reduced by allowing at least 8 weeks after prostate biopsy before performing a local evaluation by MRI.[16)]

Table 4. Examples of prostate cancer sequences (for both 3T and 1.5T systems, phased-array coil)

Imaging Method	Sequence	TR/TE	Slice Thickness	Other
(1) T2-weighted/transverse	FSE	Approx. 4,000 ms/ approx. 100 ms	3 mm	The FOV is 12 to 20 cm. Imaging is performed without gaps. The entire prostate is imaged, including the seminal vesicles.
(2) T1-weighted	FSE or GRE	FSE: approx. 400 to 700 ms/10 ms; GRE: approx. 4 ms/approx. 2 ms	3 to 4 mm	Same range as diffusion-weighted and dynamic contrast imaging. Can be performed with or without fat suppression.
(3) Diffusion-weighted	SE-EPI Concurrent fat suppression with STIR or CHESS	≥ 3,000 ms/ ≤ 90 ms	≤ 4 mm	ADC map generated with FOV of 16 to 22 cm and 2 b-values of 0 to 100 and 800 to 1,000 s/mm^2. Diffusion-weighted images with high b-values (b-values > 1400 s/mm^2) can be acquired by actual imaging or with computed DWI instead.
(4) T2-weighted/coronal or sagittal	FSE	Approx. 4,000 ms/ approx. 100 ms	3 mm	The prostate is set to be slightly caudal to the center of the FOV.
(5) Dynamic MRI, transverse plane	3D GRE Concomitant fat suppression	< 100 ms/ < 5 ms	3 mm	Temporal resolution of < 15 s is preferable, and observations are carried out through 2 min after contrast medium injection.

DWI: diffusion-weighted image

There has been large variability between facilities and radiologists with respect to imaging and image interpretation performed to detect prostate cancer. The Prostate Imaging-Reporting and Data System (PI-RADS), which was designed to standardize these procedures, was proposed in 2012, and versions 2[17] and 2.1[18] were published in 2015 and 2019, respectively. Awareness of PI-RADS is increasing in Japan. Based on the standardized imaging methods indicated by PI-RADS, example parameters for each imaging method are shown in Table 4. The parameters should be optimized by the individual institutions.

1. Preparation before an MRI examination: To obtain better images

Before an MRI examination, the patient is asked to evacuate the bowel to reduce intrarectal gas and residue, which can degrade images.

If an antispasmodic (glucagon, scopolamine butylbromide) can be used, it can reduce motion artifacts resulting from intestinal peristalsis. However, cost and adverse reactions need to be considered.

2. Magnetic field strength

Although appropriate parameters can be obtained with either a 3T or 1.5T system, imaging with a 3T system is recommended. Imaging is performed using a 1.5T system if image quality degradation is a concern due to metal artifacts from implantable devices; such as bilateral total hip replacement. Prostate MRI using a low magnetic field of < 1.5T is not recommended.

3. Signal receiving coil

Given suitable imaging conditions, appropriate images can be obtained using a phased-array coil. The use of a transrectal coil is therefore unnecessary, particularly in view of the invasiveness of such coils.

4. Prostate MRI protocol

T1-weighted, T2-weighted (≥ 2 imaging planes), diffusion-weighted, and dynamic contrast-enhanced study constitute the basic protocol. T2-weighted, diffusion-weighted, and dynamic contrast-enhanced study are particularly important for diagnosis (Fig. 3).

① T2-weighted imaging

T2-weighted imaging is performed using FSE in the transverse plane and at least 1 other plane (coronal or sagittal). A slice thickness of 3 mm without interslice gap is recommended. 3D acquisition can be used as an adjunct to 2D images. 3D acquisition with isotropic voxels enables detailed anatomical structures to be visualized and is useful for distinguishing true lesions from pseudolesions due to partial volume effects. It should be noted, however, that the soft tissue contrast of 3D images is not the same as 2D-images, and that the contrast may be inferior to that of 2D T2-weighted imaging.

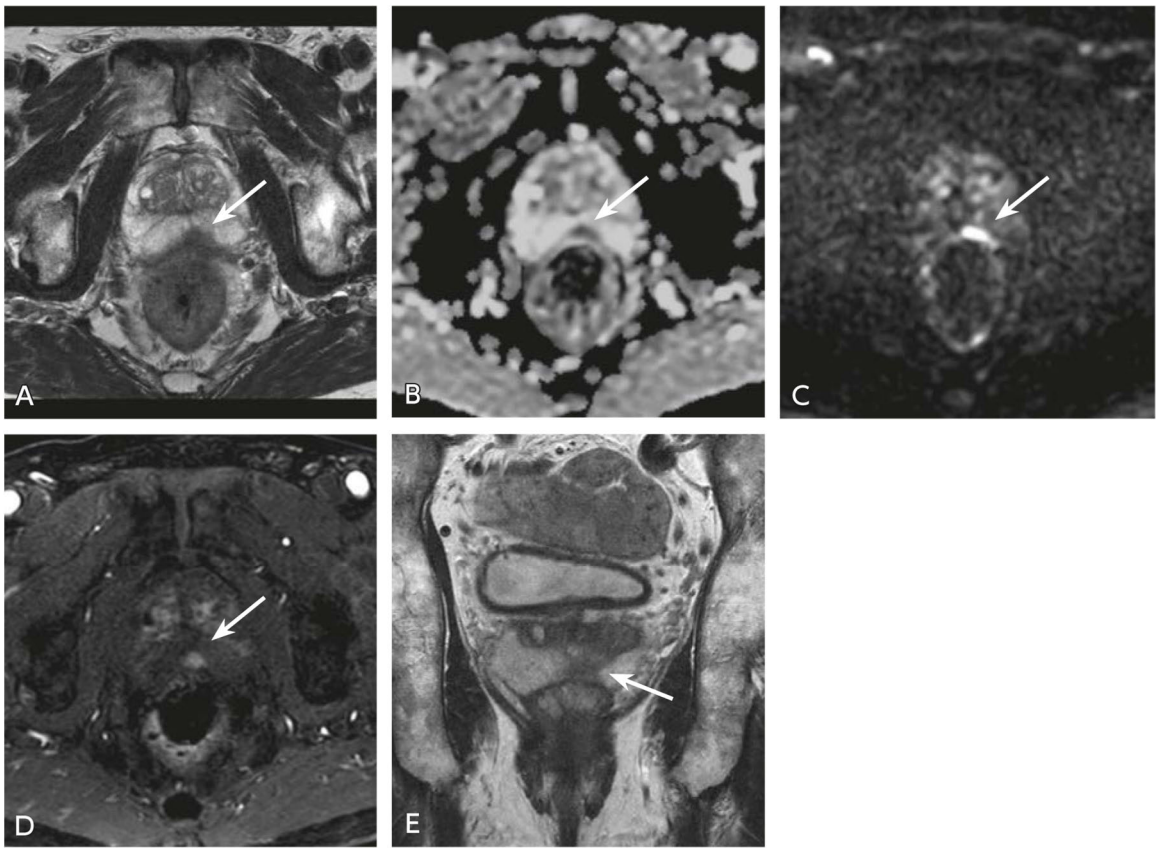

Figure 3. MRI of prostate cancer (T2a)

A: T2-weighted transverse image; B: ADC map; C: Diffusion-weighted image (b-value = 2,000 s/mm^2);
D: Dynamic contrast image, early phase; E: T2-weighted coronal image
The patient was a man in his 70s. A 10-mm nodule is seen in the margin of the left lobe of the prostate gland. The nodule shows hypointensity in the T2-weighted image (A) and ADC map (B) and early enhancement in the dynamic contrast image (C). The findings are suggestive of prostate cancer. In the T2-weighted coronal image, an area of hypointensity is seen extending caudally from the center region (D). The findings in the dynamic contrast image and T2-weighted coronal image facilitate differentiation of the normal central region from the cancer. It should be noted that intrarectal gas can distort diffusion-weighted images and make it difficult to evaluate the dorsal portion of the prostate.

② Diffusion-weighted imaging

For diffusion-weighted imaging, SE-EPI (with fat suppression) and normal breathing are recommended. Matching of slice location and slice thickness of T2-weighted imaging facilitates diagnosis. Diffusion-weighted imaging with a high b-value (b-value > 1,400 s/mm^2) and ADC map are required. The ADC map must be generated from a low b-value (0 to 100 s/mm^2) and an intermediate b-value (800 to 1,000 s/mm^2). Consequently, if there is a limitation with respect to time or another factor, one possible approach is to acquire imaging with only low and intermediate b-values and compute DWI with a high b-value.

③ T1-weighted imaging

Transverse plane images are acquired using SE and GRE. Fat suppression may or may not be used. Hemorrhage in the prostate gland or the seminal vesicle can be detected. The imaging range can be the

same as with diffusion-weighted and dynamic contrast-enhanced study. However, because high spatial resolution is not necessary for T1-weighted images as T2-weighted imaging, it can be modified to reduce the acquisition time or to increase the imaging range. In at least 1 plane, the area from the inferior margin of the prostate to the common iliac bifurcation is included in the imaging range, and the lymph nodes present at the cranial end of the prostate are evaluated.

④ Dynamic contrast imaging

For dynamic contrast imaging, fat-suppressed GRE T1-weighted imaging is performed. A 3D sequence (e.g., VIBE, LAVA, THRIVE) is recommended. An FOV that includes the prostate and seminal vesicles in their entirety is selected. Spatial resolution should be ≤ 2 mm × 2 mm and temporal resolution < 15 s. Observation is carried out for 2 min after contrast medium injection. If any signal change such as post-biopsy hemorrhage is seen as hyperintensity on T1-weighted imaging before contrast-enhanced imaging, subtraction images facilitate determination of the presence or absence of contrast enhancement.

Metastasis could be found if the prostate specific antigen (PSA) level is ≥ 10 ng/mL or the Gleason score for cancer tissue obtained by biopsy is ≥ 8. Consequently, in addition to prostate MRI, which is a local evaluation, CT is performed for whole-body metastasis screening, and bone scintigraphy is performed to assess bone metastasis.

Imaging methods for the testicles and scrotum

Testicular and scrotal lesions are broadly classified as those associated with acute symptoms referred to as acute scrotum and those not associated with such symptoms. The former type includes testicular torsion, testicular infarction, acute epididymo-orchitis, and testicular rupture. The latter includes tumor, granuloma, and testicular microlithiasis. Many testicular tumors are detected due to irregular nodular swelling found by self-examination. More than 90% of testicular tumors are malignant germ cell tumors that occur in relatively young men between the ages of approximately 15 and 45 years. The other types of tumors include sex cord-stromal tumors, malignant lymphoma, leukemia, and metastatic tumors.

Ultrasonography is the first choice of diagnostic imaging modalities for testicular and scrotal lesions, with Doppler ultrasonography used concomitantly to evaluate blood flow. Ultrasonography is also the first choice for acute scrotum. However, difficulty may be encountered in evaluating testicular blood flow by ultrasonography, and dynamic MRI using a contrast medium is added in that case. If a tumorous lesion is suspected, MRI can be used to identify intratumoral hemorrhage, necrosis, and the fatty component, and to sensitively evaluate structures such as septal structures. Ultrasonography and MRI can be used in combination for purposes such as differentiating between benign and malignant lesions, inferring the histopathological-type of tumors, and evaluating aspects such as local progression. To diagnose the distant metastasis of tumorous lesions, evaluation by CT, MRI, or radioisotope inspection (RI, PET) is performed.

1. MRI of testicular and scrotal lesions[19)]

Because of the small size of the imaging target, high-resolution imaging is necessary. An MR scanner of 1.5T or higher should be used.

A 3T scanner, which provides a better SNR than 1.5T, should be used if possible. However, scientific evidence that 3T systems are more useful is lacking. The receiver coil used is a surface or phased-array coil, each of which has a high SNR and enables high-resolution imaging.

The field-of-view (FOV) includes the bilateral scrotum, and the transverse and coronal plane imaging indicated below is performed with a small FOV and thin slice thickness (FOV: approximately 15 to 20 cm; slice thickness: approximately 3 to 5 mm; slice gap: minimum).

T1- and T2-weighted imaging are standard. In the case of tumorous lesions, fat-suppressed T1-weighted imaging or dual echo T1-weighted imaging is added to detect the fatty component occasionally seen in germ cell tumors. For acute scrotum, $T2^*$-weighted imaging, which sensitively detects the intratesticular hemorrhage seen with testicular torsion, is added as needed.

Diffusion-weighted imaging is recommended because it reflects the pathological background of lesions. The imaging is performed with b-values of at least 0 s/mm^2 and 800 to 1,000 s/mm^2, and an ADC map is generated. Lesions such as epidermoid cysts and seminomas and malignant lymphomas, which have high cellularity, show particularly marked hyperintensity in diffusion-weighted images, which is useful for differentiation (Fig. 4).

Dynamic contrast MRI is an important imaging method for acute scrotum in particular. Using 3D GRE T1-weighted imaging, a gadolinium contrast medium is rapidly injected intravenously, and imaging is performed approximately 30 s to 1 min later. This is done repeatedly, and the contrast enhancement of areas such as the testicles and epididymis is assessed (Fig. 5). Imaging should be performed until 8 min after injection to assess washout from tumorous lesions. If visually assessing contrast enhancement is difficult, subtraction images are generated, and time-signal intensity curves are plotted for the testicles and lesions. In the case of a tumorous lesion, dynamic contrast MRI can be omitted, and aspects such as the internal structure and extent of progression can be evaluated with normal pre- and post-contrast T1-weighted imaging alone (or fat-suppressed contrast T1-weighted imaging).

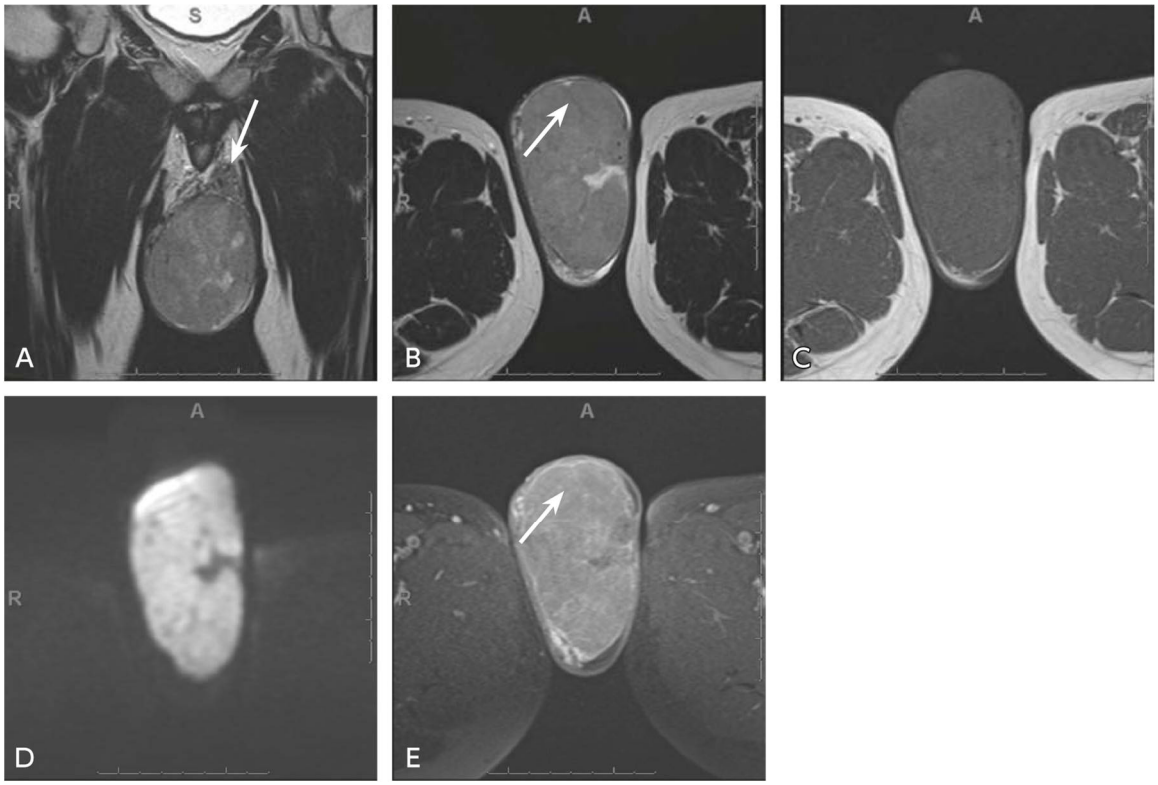

Figure 4. MRI of a malignant testicular tumor

A: T2-weighted coronal image; B: T2-weighted transverse image; C: T1-weighted image; D: Diffusion-weighted image; E: Post-contrast image

The left testis is enlarged and replaced by a tumor of moderate signal intensity in the T2-weighted images. The interior is relatively homogeneous and shows a signal of moderate intensity in the T2-weighted images and marked hyperintensity in the diffusion-weighted image. Extension to the spermatic cord is visualized in the coronal T2-weighted image (A →). In addition, a restiform structure that shows hypointensity on T2-weighted imaging (B →) is seen in the interior, with increased contrast enhancement of this structure seen (E →). The findings reflect fibrous septa, and a seminoma is strongly suspected.

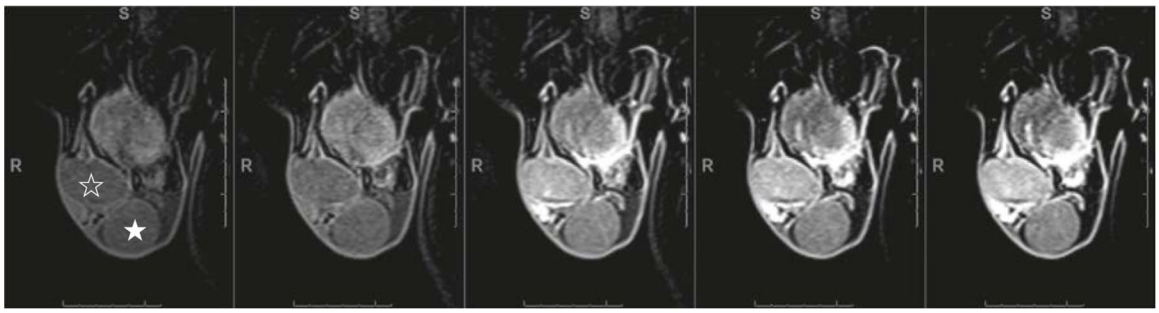

Figure 5. MRI of acute scrotum

Testicular torsion was suspected but could not be confirmed by ultrasonography, and the patient underwent MRI.

Dynamic contrast MRI: No abnormalities could be identified on T1- and T2-weighted imaging (not shown). With dynamic contrast MRI, enhancement was poorer in the left testis (★) than in the right (☆). The patient underwent orchidopexy for incomplete testicular torsion, which was cured without testicular necrosis.

2. Malignant testicular tumor staging and diagnosis of recurrence

Malignant testicular tumors tend to metastasize to the lymph nodes and lungs. With regard to lymph node metastasis, tumors that arise in the left testis metastasize to the lateral side of the aorta near the left renal vein. Right testicular tumors progress from the pericaval lymph nodes at the height of the 2nd lumbar vertebra to the thoracic duct and metastasize to the left supraclavicular lymph nodes and lungs. Infiltration of the epididymis by the primary tumor increases the risk of metastasis to the inguinal lymph nodes. Hematogenous metastasis often occurs in the late stage of the disease. However, choriocarcinoma metastasizes to the lungs early and may also metastasize to the brain, bone, and liver. Contrast-enhanced CT, which enables high-speed, extensive imaging using thin slices, is useful for evaluating such lymph node and pulmonary metastases.

For the contrast medium, a 300 mgI/mL nonionic contrast agent is administered at an injection rate of 2 to 3 mL/s. The volume administered is either approximately 100 mL or approximately 2 mL per kilogram of the patient's weight. The timing of the imaging is approximately 50 to 60 s after the start of contrast medium administration. The area imaged is from the supraclavicular fossa to the inguinal region. Reconstruction using a slice thickness of ≤ 5 mm is recommended. Although the cutoff value for lymph node enlargement is generally a short-axis diameter of 10 mm, a short-axis diameter of approximately 6 mm and the use of thin slices are necessary to evaluate lymph node metastases of testicular tumors.[20)]

As necessary, bone scintigraphy is performed to evaluate bone metastasis, and contrast-enhanced MRI is performed to evaluate brain metastasis. In addition, FDG-PET has been reported to be useful for lymph node, pulmonary, and bone metastases. However, as indicated for BQ76, there is inadequate scientific evidence to recommend PET alone.

The frequency of recurrence varies according to factors such as the stage, histopathological type, and recurrence risk classification, and the timing for performing each type of imaging examination for posttreatment follow-up also varies. In this regard, the European Association of Urology (EAU) guidelines[21)] and the National Comprehensive Cancer Network (NCCN) Clinical Practice Guidelines in Oncology[22)] are instructive.

Secondary source materials used as references

1) Sheth S et al: Current concepts in the diagnosis and management of renal cell carcinoma: role of multidetector CT and three-dimensional CT. Radiographics 21: S237-254, 2001
2) Pedrosa I et al: MR imaging of renal masses: correlation with findings at surgery and pathologic analysis. Radiographics 28: 985-1003, 2008
3) Vendrami CL et al: Differentiation of solid renal tumors with multiparametric MR imaging. Radiographics 37: 2026-2042, 2017
4) Urban BA et al: Tailored helical CT evaluation of acute abdomen. Radiographics 20: 725-749, 2000
5) Stunell H et al: Imaging of acute pyelonephritis in the adult. Eur Radiol 17: 1820-1828, 2007
6) Van Der Molen AJ et al: CT urography: definition, indications and techniques: a guideline for clinical practice. Eur Radiol 18: 4-17, 2008
7) Jinzaki M et al: Role of computed tomography urography in the clinical evaluation of upper tract urothelial carcinoma. Int J Urol 23: 284-298, 2016
8) Akita H et al: Performance of diffusion-weighted MRI post-CT urography for the diagnosis of upper tract urothelial carcinoma: Comparison with selective urine cytology sampling. Clin Imaging 52: 208-215, 2018

9) Akita H et al: Preoperative T categorization and prediction of histopathologic grading of urothelial carcinoma in renal pelvis using diffusion-weighted MRI. AJR Am J Roentgenol 197: 1130-1136, 2011
10) Japan Radiological Society, Ed.: Diagnostic Imaging Guidelines 2016. KANEHARA & Co., 2016.
11) Japanese Urological Association, Ed.: 2019 Clinical Practice Guidelines for Bladder Cancer. Igakutosho Shuppan, 2019.
12) Sudakoff GS et al: Multidetector computerized tomography urography as the primary imaging modality for detecting urinary tract neoplasms in patients with asymptomatic hematuria. J Urol 179: 862-867, 2008
13) Kim JK et al: Bladder cancer: analysis of multi-detector row helical CT enhancement pattern and accuracy in tumor detection and perivesical staging. Radiology 231: 725-731, 2004
14) Jinzaki M et al: Detection of bladder tumors with dynamic contrast-enhanced MDCT. AJR Am J Roentgenol 188: 913-918, 2007
15) Panebianco V et al: Multiparametric magnetic resonance imaging for bladder cancer: development of VI-RADS (Vesical Imaging-Reporting and Data System). Eur Urol 74: 294-306, 2018
16) Qayyum A et al: Organ-confined prostate cancer: effect of prior transrectal biopsy on endorectal MRI and MR spectroscopic imaging. AJR Am J Roentgenol 183: 1079-1083, 2004
17) Weinreb JC et al: PI-RADS (Prostate Imaging-Reporting and Data System) version 2. Eur Urol 69: 16-40, 2015
18) Turkbey B et al: PI-RADS (Prostate Imaging-Reporting and Data System) version 2.1. Eur Urol 76: 340-351, 2019
19) Tsili AC et al: MRI of the scrotum: recommendations of the ESUR scrotal and penile imaging working froup. Eur Radiol 28: 31-43, 2018
20) Hilton S et al: CT detection of retroperitoneal lymph node metastases in patients with clinical stage I testicular non seminomatous germ cell cancer: assessment of size and distribution criteria. AJR Am J Roentgenol 169: 521-525, 1997
21) Albers P et al: Guidelines on testicular cancer: 2015 Update. Eur Urol 68: 1054-68, 2015
22) Gilligan T et al: NCCN clinical practice guidelines in oncology: testicular cancer version 2. J Natl Compr Canc Netw 17: 1529-1554, 2019

BQ 68 Is DMSA scintigraphy recommended to detect renal scarring?

Statement

DMSA scintigraphy is useful and recommended for detecting renal scarring.

Background

Repeated recurrence of pyelonephritis due to vesicoureteral reflux or upper urinary tract infection is known to result in impairment and scarring of the renal parenchyma. Scarring can also occur as a result of conditions such as asymptomatic congenital hydronephrosis. Extensive scarring can cause decreased kidney function, resulting in conditions such as proteinuria, hypertension, and renal failure. Consequently, early detection is required. To detect renal scarring, ultrasonography and dimercaptosuccinic acid (DMSA) are often used. For this BQ, the usefulness of renal scarring detection by DMSA scintigraphy was examined.

Explanation

Farghaly et al. performed DMSA planar imaging and SPECT imaging in 190 patients with conditions such as vesicoureteral reflux. Of the 200 examinations performed, scarring was detected in 95 planar imaging examinations and 100 SPECT examinations.[1)]

Temiz et al. compared the results of DMSA scintigraphy and ultrasonography in 62 pediatric patients (mean age, 5 years; range, 6 months to 15 years) with vesicoureteral reflux. Although DMSA scintigraphy detected scarring in 55%, the detection rate was 38% with ultrasonography. Moreover, DMSA scintigraphy was able to identify scarring in 35% of kidneys deemed normal by ultrasonography.[2)]

Brenner et al. compared DMSA planar images and SPECT images of 40 patients (37 of whom were children). They found no significant difference in the number of scars detected by the 2 methods.[3)]

Moorthy et al. examined the kidneys of 930 children who underwent ultrasonography and DMSA examinations on the same day. They found that, although ultrasonography provided high specificity in detecting renal scarring, its sensitivity and positive and negative predictive values were low. They concluded that ultrasonography cannot substitute for DMSA examination.[4)]

Moreover, DMSA scintigraphy can enable quantitation by expressing the rate of renal tracer uptake as a percentage, providing a useful index for the evaluation and follow-up of renal function.

Search keywords and secondary sources used as references

PubMed was searched using the following keywords: renal, scar, DMSA, and detection. Four articles were selected from the results.

1) Farghaly HRS, Mohamed Sayed MH: Technetium-99m dimercaptosuccinic acid scan in evaluation of renal cortical scarring: Is it mandatory to do single photon emission computerized tomography? Indian J Nucl Med 30 (1): 26-30, 2015

2) Temiz Y et al: The efficacy of Tc99m dimercaptosuccinic acid (Tc-DMSA) scintigraphy and ultrasonography in detecting renal scars in children with primary vesicoureteral reflux (VUR). Int Urol Nephrol 38 (1): 149-152, 2006
3) Brenner M et al: Comparison of 99mTc-DMSA dual-head SPECT versus high-resolution parallel-hole planar imaging for the detection of renal cortical defects. AJR Am J Roentgenol 193 (2): 333-337, 2009
4) Moorthy I et al: Ultrasonography in the evaluation of renal scarring using DMSA scan as the gold standard. Pediatr Nephrol 19 (2): 153-156, 2004

BQ 69 Is contrast-enhanced CT recommended to evaluate solid renal masses?

Statement

Contrast-enhanced CT is strongly recommended to determine whether a renal mass is solid.

Dynamic CT is recommended because it can identify clear cell renal cell carcinomas, which account for 70% to 80% of renal cell carcinomas (RCCs), and because benign disease, for which surgery is omitted, can be suspected if enhancement of the mass is homogeneous.

Background

Diagnosis of a solid renal tumor involves first determining that it is a solid mass. Next, benign masses are differentiated from malignant ones. Based on disease frequency, it is important to differentiate renal cell carcinoma (RCC) from renal angiomyolipoma (AML) and oncocytoma. In the case of a malignancy, information on tissue-type should also be provided. For the purpose of molecularly targeted therapy, it is also now important to differentiate between clear cell renal cell carcinoma and other tissue-types. The following discussion provides an overview regarding the usefulness of contrast-enhanced CT for identifying solid renal masses, differentiating benign from malignant masses, and diagnosing the subtype of a mass.

Explanation

Characterizing a mass as solid or cystic involves performing not only non-contrast CT, but also contrast-enhanced CT imaging, and observing the presence or absence of contrast enhancement is very important. In the past, a mass was judged to be solid when an increase in the CT number of ≥ 10 HU was seen from pre- to post-contrast.[1)] However, since the emergence of helical CT, in view of the pseudoenhancement effect, an increase in the CT number of ≥ 20 HU has been considered to indicate contrast enhancement.[2)] Moreover, characterizing masses ≤ 10 mm in size is difficult with a slice thickness of 5 mm. However, imaging with thin slices of approximately 3 mm markedly improves the characterization of 5 to 10 mm masses.[3)] If a cyst is strongly suspected at the non-contrast CT stage, normal contrast-enhanced CT (nephrographic phase) is adequate. However, if a solid mass is suspected, dynamic CT is recommended to differentiate a benign mass from a malignant mass.

Because the proportion of resected masses that are benign is 46.3% for those < 1 cm in size and approximately 20% for those 2 to 4 cm in size, rigorously distinguishing malignant tumors from others is particularly important for preoperatively evaluating small-diameter tumors.[4)] AML can often be diagnosed by detecting the fat concentrations (< -10 HU) with non-contrast CT. This is referred to as classic AML. Non-contrast CT is more accurate than contrast-enhanced CT for detecting fat concentrations.[5)] In comparison, the homogeneity and contrast pattern of contrast-enhanced CT are useful for differentiating

fat-poor AML[6], which accounts for approximately 5% of AMLs, from RCC.[7] First, masses that show non-homogeneous marked enhancement in the corticomedullary phase of dynamic CT can be almost definitively determined to be clear cell renal cell carcinomas, i.e., malignant (Fig. 1).[8-10] However, few fat-poor AMLs show early-phase enhancement. Rather, many show homogeneous mild to moderate enhancement (Fig. 2).[6, 7, 11, 12] In addition, hyperdensity (≥ 45 HU) compared with the renal parenchyma[6, 7, 13, 14] and tumors with a higher long-axis diameter/short-axis diameter ratio on non-contrast CT are common.[13] Oncocytomas, although known for central scarring, show homogeneity on contrast-enhanced CT if small in size. The contrast pattern of oncocytomas resembles that of chromophobe renal cell carcinomas, which tends to be homogeneous, which poses a problem for their differentiation. Segmental enhancement inversion (tumor more strongly enhanced in the early phase of contrast than in the late phase; converse true for the interstitium) has been proposed as a characteristic finding of oncocytomas. However, this finding has also been reported for chromophobe renal cell carcinomas. Consequently, differentiating oncocytomas from chromophobe renal cell carcinomas remains difficult. In addition, benign tumors such as leiomyomas and metanephric adenomas also show hyperintensity on non-contrast CT and homogeneity on contrast-enhanced CT. Hyperdensity and homogeneous contrast on non-contrast CT (hyperattenuating homogeneously enhancing masses) are useful clues that suggest a possibly benign mass.[6, 7, 11] However, malignancies such as papillary renal cell carcinomas also have this appearance, and a definitive determination by biopsy is therefore recommended.[6, 7, 11]

Figure 1. Clear cell renal cell carcinoma

Contrast-enhanced CT, corticomedullary phase: A non-homogeneously enhancing mass is seen in the left kidney (→), a finding indicative of clear cell renal cell carcinoma.

Figure 2. Fat-poor AML

Contrast-enhanced CT, corticomedullary phase: A homogeneous and hypovascular solid mass is seen in the right kidney (→). The mass is a fat-poor AML.

Dynamic CT is also useful for diagnosing RCC subtypes. The 3 main RCC tissue types are the clear cell, chromophobe, and papillary types. Clear cell renal cell carcinomas undergo non-homogeneous enhancement in the corticomedullary phase and decreased enhancement in the nephrographic and early

excretory phases.[8-10] Chromophobe renal cell carcinomas show moderate homogeneous contrast enhancement in the corticomedullary phase and decreased enhancement subsequently.[8-10] Papillary renal cell carcinomas often undergo only slight contrast enhancement in the corticomedullary phase and gradual homogeneous enhancement.[8-10] These differences in contrast patterns reflect intratumoral angiogenesis,[8] and the 3 main tissue types can be mutually differentiated. It should be noted, however, that oncocytomas show similar enhancement pattern with clear cell renal cell carcinomas and chromophobe renal cell carcinomas[8-10, 15-17], and that metanephric adenomas resemble papillary renal cell carcinomas.[8]

Search keywords and secondary sources used as references

PubMed was searched using the following keywords: renal, tumor, CT, assessment, characteristics, differentiation, pathologic correlation, renal cell carcinoma, and angiomyolipoma.

In addition, the following was referenced as a secondary source.

1) Wang ZJ et al: ACR Appropriateness Criteria®: clinical condition indeterminate renal masses. J Am Coll Radiol 17: S415-S428, 2020

References

1) Bosniak MA: The small (less than or equal to 3.0 cm) renal parenchymal tumor: detection, diagnosis, and controversies. Radiology 179: 307-317, 1991
2) Curry NS: Small renal masses (lesions smaller than 3 cm): imaging evaluation and management. AJR Am J Roentgenol 164: 355-362, 1995
3) Jinzaki M et al: Evaluation of small (＜/＝3 cm) renal masses with MDCT: benefits of thin overlapping reconstructions. AJR Am J Roentgenol 183: 223-228, 2004
4) Frank I et al: Solid renal tumors: an analysis of pathological features related to tumor size. J Urol 170: 2217-2220, 2003
5) Davenport MS et al: Diagnosis of renal angiomyolipoma with hounsfield unit thresholds: effect of size of region of interest and nephrographic phase imaging. Radiology 260: 158-165, 2011
6) Jinzaki M et al: Angiomyolipoma: imaging findings in lesions with minimal fat. Radiology 205: 497-502, 1997
7) Jinzaki M et al: Renal angiomyolipoma: a radiological classification and update on recent developments in diagnosis and management. Abdom Imaging 39: 588-604, 2014
8) Jinzaki M et al: Double-phase helical CT of small renal parenchymal neoplasms: correlation with pathologic findings and tumor angiogenesis. J Comput Assist Tomogr 24: 835-842, 2000
9) Zhang J et al: Solid renal cortical tumors: differentiation with CT. Radiology 144: 494-504, 2007
10) Pierorazio PM et al: Multiphasic enhancement patterns of small renal masses (≤ 4 cm) on preoperative computed tomography: utility for distinguishing subtypes of renal cell carcinoma, angiomyolipoma, and oncocytoma. Urology 81: 1265-1271, 2013
11) Silverman SG et al: Hyperattenuating renal masses: etiologies, pathogenesis, and imaging evaluation. Radiographics 27: 1131-1143, 2007
12) Yang CW et al: Are there useful CT features to differentiate renal cell carcinoma from lipid-poor renal angiomyolipoma? AJR Am J Roentgenol 201: 1017-1028, 2013
13) Woo S et al: Angiomyolipoma with minimal fat and non-clear cell renal cell carcinoma: differentiation on MDCT using classification and regression tree analysis-based algorithm. Acta Radiol 55: 1258-1269, 2014
14) Schieda N et al: Unenhanced CT for the diagnosis of minimal-fat renal angiomyolipoma. AJR Am J Roentgenol 203: 1236-1241, 2014
15) Kim JI et al: Segmental enhancement inversion at biphasic multidetector CT: characteristic finding of small renal oncocytoma. Radiology. 252: 441-448, 2009
16) Schieda N et al: Diagnostic accuracy of segmental enhancement inversion for the diagnosis of renal oncocytoma using biphasic computed tomography (CT) and multiphase contrast-enhanced magnetic resonance imaging (MRI). Eur Radiol 24: 2787-2794, 2014
17) Choudhary S et al: Renal oncocytoma: CT features cannot reliably distinguish oncocytoma from other renal neoplasms. Clin Radiol 64: 517-522, 2009

FQ 16 In which cases is MRI recommended to differentiate renal mass lesions?

Statement

MRI is useful when determining whether a lesion is benign or malignant is difficult with CT and when differentiating RCC subtypes. MRI is also used when contrast-enhanced CT cannot be performed due to circumstances such as pregnancy, decreased renal function, or allergy to iodinated contrast media.

Background

Recently, the frequency with which small renal masses ≤ 4 cm in diameter are detected incidentally on ultrasonography and CT has increased. Because it is known that the frequency of benign masses increases among those ≤ 4 cm in diameter, differentiating benign from malignant masses is critical.[1)] Multiparametric MRI (mpMRI) is a concept that involves analyzing image data as qualitative, semi-quantitative, and quantitative biomarkers. The data are for images such as T1-weighted images (chemical shift images: in-phase and opposed-phase images), T2-weighted images, diffusion-weighted images, and dynamic contrast images.[2)] In fact, mpMRI of renal mass lesions is considered useful for the qualitative diagnosis of lesions (benign-malignant differentiation), as well as their detection, and for differentiating RCC subtypes.[1)]

Explanation

The most common type of small solid renal mass for which surgery is performed is malignant RCC (~ 80%). The main subtypes are the clear cell, papillary, and chromophobe types, with frequencies of 75%, 10%, and 5%, respectively. The clear cell type has a poor prognosis.[2)] The diagnostic accuracy rate of CT in diagnosing solid renal masses as RCC is ≥ 90%.[3)] Consequently, a general treatment strategy can be determined using CT examinations in nearly all cases. On the other hand, the frequency of benign tumors has been reported to be 46.3% for those < 1 cm in size and 20% for those 2 to 4 cm in size, the main tumors being renal AMLs and oncocytomas.[4)] As background, the frequency of identified benign masses is lower in Asian, including Japanese, populations than in European and American populations. This is because oncocytomas are less frequent in the Asian population, and angiomyolipomas account for a relatively large number.[5, 6)] Ninety-five percent of AMLs are classic AMLs, in which the fat component of the mass can be detected by CT (CT number < -10 HU). However, approximately 5% are fat-poor AMLs, in which fat cannot be detected. Consequently, differentiating AMLs from RCCs by CT alone is often difficult.[7)] Oncocytomas have characteristic findings, such as early-phase contrast enhancement that ranges from moderate to hypervascular,[8)] central scarring, and segmental enhancement inversion. However, these findings are also seen with RCC,[9)] making diagnosis by CT alone difficult. Consequently, it is expected that

the addition of MRI for indeterminate renal masses to assess them as benign or malignant on CT could improve differentiation accuracy.[1)]

First, tumors that show post-contrast homogeneous enhancement on CT may be benign. Of these, those that show hyperdensity comparable to that of skeletal muscle on non-contrast CT and hypointensity on T2-weighted images are strongly suspected of being fat-poor AMLs (hyperattenuating type).[7, 10)] Such tumors often show low values in ADC maps, early-phase contrast enhancement, and late-phase washout.[10)] For tumors that show attenuation comparable to that of the renal parenchyma and mild-to-moderate, homogeneous early-phase contrast enhancement on non-contrast CT, a fat-poor AML (iso-attenuating type) is suspected if the tumor shows a lower signal on T1-weighted opposed-phase images than on in-phase images.[7)] However, although an examination of the use of mpMRI for renal masses with central scarring seen by CT showed that it may be possible to use MRI to exclude oncocytoma,[11)] it is difficult to diagnose actively on MRI. In addition, differentiating homogeneous oncocytomas from renal cell carcinoma is also considered difficult even with the use of mpMRI.[1)]

Furthermore, mpMRI may be useful for diagnosing RCC subtypes. If a tumor shows attenuation comparable to that of the renal parenchyma on non-contrast CT, mild early-phase contrast enhancement, and gradually increasing late-phase enhancement, papillary renal cell carcinoma is most commonly suspected based on frequency. With the addition of MRI in this case, a low signal in T2-weighted images is suggestive of papillary renal cell carcinoma,[10)] and a moderate-to-high signal indicates a possible mucinous tubular and spindle cell carcinoma.[11)] Papillary renal cell carcinomas often show a decreased signal on in-phase T1-weighted images compared with opposed-phase T1-weighted images due to intratumoral hemorrhage.[12)] In comparison, due to intracellular lipids, clear cell renal cell carcinomas show a lower signal on opposed-phase T1-weighted images than on in-phase images, a non-homogeneous high signal in T2-weighted images, and early-phase non-homogeneous enhancement.[1)]

CT is readily accessible and less expensive than MRI, and a single CT examination can provide information for the qualitative diagnosis of renal masses and staging over an extensive area and on structures such as the renal artery and vein and ureter. Consequently, as the first-choice examination, CT is highly useful. Another advantage of CT is that it is suitable for use in elderly individuals and patients who cannot tolerate a long examination duration or breath-hold examination.[14)] MRI, on the other hand, does not involve exposure to ionizing radiation, and it can visualize lesions with tissue contrast superior to that of CT. The diagnostic performance of MRI for detecting lesions that require surgery and locally staging RCC compares favorably with CT. However, many facilities have busy MRI examination schedules, and few can perform emergency examinations. In addition, due to considerations such as the somewhat higher fees for MRI than for CT and the long duration of MRI examinations, MRI is performed as an adjunct subsequent to CT. However, MRI is the first examination used in circumstances where contrast-enhanced CT cannot be performed, as in pregnancy, decreased renal function, or allergy to iodinated contrast media.[15)]

Although CT plays the central role in the diagnostic imaging of solid renal masses, MRI may be useful for differentiating benign from malignant masses and diagnosing renal cell carcinoma subtypes when used as an adjunctive examination. It can also aid in determining a treatment plan.

Search keywords and secondary sources used as references

PubMed was searched using the following keywords: renal tumors, renal cell carcinoma, oncocytoma, angiomyolipoma, and MRI. The period searched was through June 2019.

In addition, the following were referenced as secondary sources.

1) Japan Radiological Society, Ed.: Diagnostic Imaging Guidelines 2016. KANEHARA & Co., 2016.
2) Heilbrun ME et al: ACR Appropriateness Criteria®: indeterminate renal mass. J Am Coll Radiol 12: 333-341, 2015

References

1) Vendrami CL et al: Differentiation of solid renal tumors with multiparametric MR imaging. Radiographics 37: 2026-2042, 2017
2) Kay FU et al: Imaging of solid renal masses. Radiol Clin North Am 55: 243-258, 2017
3) Kim EY et al: Clinico-radio-pathologic features of a solitary solid renal mass at MDCT examination. Acta Radiol 51: 1143-1148, 2010
4) Frank I et al: Solid renal tumors: an analysis of pathological features related to tumor size. J Urol 170: 2217-2220, 2003
5) Fujii Y et al: Incidence of benign pathologic lesions at partial nephrectomy for presumed RCC renal masses: Japanese dual-center experience with 176 consecutive patients. Urology 72 (3): 598-602, 2008
6) Fujii Y et al: Benign lesions at surgery for presumed renal cell carcinoma: an Asian perspective. Int J Urol 17 (6): 500, 2010
7) Jinzaki M et al: Renal angiomyolipoma: a radiological classification and update on recent developments in diagnosis and management. Abdom Imaging 39: 588-604, 2014
8) Cornelis F et al: Routinely performed multiparametric magnetic resonance imaging helps to differentiate common subtypes of renal tumours. Eur Radiol 24: 1068-1080, 2014
9) Rosenkrantz AB et al: MRI Features of renal oncocytoma and chromophobe renal cell carcinoma. AJR Am J Roentgenol 195: W421-427, 2010
10) Lim RS et al: Renal angiomyolipoma without visible fat: can we make the diagnosis using CT and MRI? Eur Radiol 28: 542-553, 2018
11) Cornelis F et al: Combined late gadolinium-enhanced and double-echo chemical-shift MRI help to differentiate renal oncocytomas with high central T2 signal intensity from renal cell carcinomas. AJR Am J Roentgenol 200: 830-838, 2013
12) Chiarello MA et al: Diagnostic accuracy of MRI for detection of papillary renal cell carcinoma: a systematic review and meta-analysis. AJR Am J Roentgenol 211: 812-821, 2018
13) Cornelis F et al: CT and MR imaging features of mucinous tubular and spindle cell carcinoma of the kidneys: a multi-institutional review. Eur Radiol 27: 1087-1095, 2017
14) Krishna S et al: CT imaging of solid renal masses: pitfalls and solutions. Clin Radiol 72: 708-721, 2017 15) Allen BC et al: Characterizing solid renal neoplasms with MRI in adults. Abdom Imaging 39: 358-387, 2014
15) Allen BC et al: Characterizing solid renal neoplasms with MRI in adults. Abdom Imaging 39: 358-387, 2014

BQ 70 Which imaging examinations are recommended for staging renal cancer?

Statement

Contrast-enhanced CT is strongly recommended. MRI is the alternative modality for patients who cannot undergo contrast-enhanced CT. MRI may be useful if determining the presence or absence of perirenal fat invasion, intravenous tumor thrombus, and venous mural infiltration of tumor thrombus is difficult with CT.

Chest CT is recommended if there is a risk of pulmonary metastasis due to a very large primary tumor or locally advanced disease. Chest radiography is recommended if the risk of pulmonary metastasis is low.

Bone scintigraphy is not recommended as a routine examination. It can be considered if bone metastasis is clinically suspected.

PET has been reported to be useful for metastasis screening and diagnosing recurrence during follow-up. However, its significance as a routine examination has not been established.

Background

Preoperative staging of renal cancer is essential for formulating a treatment plan. As indicated in The General Rule for Clinical and Pathological Studies on Renal Cell Carcinoma, the modality that plays the central role in this is CT. Evidence regarding the usefulness of incorporating MRI, bone scintigraphy, and PET is also reviewed.

Explanation

1. CT

In a prospective study of imaging methods, the staging capability of CT was significantly greater with combined 3-phase imaging (plain, corticomedullary phase, and nephrographic phase: diagnostic accuracy rate, 91%) than with combined 2-phase imaging (plain and corticomedullary phase or plain and nephrographic phase: diagnostic accuracy rate, 82% and 86%, respectively).[1)] Dynamic contrast CT is considered useful both for the qualitative diagnosis of masses and for staging.

The biggest factor that has reduced the staging capability for the T stage of renal cancers has been low diagnostic performance for perirenal and renal sinus fat invasion (differentiation of T1/T2 and T3a).[1-5)] CT findings of perirenal fat invasion include the following: renal fascial thickening, thickening of the bridging septa, fluid accumulation, left-right asymmetrical dilatation and irregularity of the peritumoral blood vessels and blood vessels in Gerota's fascia, the presence of tumorous nodules in the tumor margins and perirenal fatty space, and contrast enhancement of those nodules.[6, 7)] The General Rule for Clinical and Pathological Studies on Renal Cell Carcinoma indicates that outward protrusion from the renal contour

resulting in rupture of the lateral cortex and nodules ≥ 1 cm in size that are continuous with tumors in perirenal fatty tissue should be evaluated. However, difficulty may be encountered in differentiating tumor infiltration and benign changes in fatty tissue resulting from conditions such as inflammation. The reported sensitivity and specificity of CT for perirenal fat invasion ranged from 84% to 100% and from 56% to 93%, respectively.[7-9] The diagnostic performance of 16- and 64-row MDCT with respect to renal sinus fat invasion has also been examined. However, the positive predictive value has been found to be low, ranging from 48.9% to 56.3%, even when coronal reconstructed images were combined.[10] An investigation by Kim et al. found that CT findings that were predictors of renal sinus fat invasion were tumor diameter (≥ 5 cm), poor contrast of the lesioned kidney, irregular tumor margin, and lymph node metastasis.[10] Clinically, total nephrectomy is indicated for T1, T2, and T3a, with the exception of some T1a patients for whom partial nephrectomy is indicated. Consequently, accurate preoperative diagnosis of perirenal and renal sinus fat invasion is not of great importance. However, because arteries, veins, and lymph ducts are present in abundance in renal sinus fat, systemic metastasis is a possibility, and renal sinus fat invasion has been found to be a prognostic factor for recurrence-free survival and cancer-specific survival.[11]

The diagnostic performance of CT with respect to intravenous tumor thrombus has been found to improve with the use of multiplanar reconstruction images, with sensitivity and specificity of 93% and 80%, respectively, which have been reported as measures of its detection performance.[12] CT has been found to be capable of identifying the extent of tumor thrombus with accuracy of 84%, with the exception of the segmental veins.[13]

Although the diagnostic criteria used for lymph node metastasis are generally a short-axis diameter ≥ 1 cm with loss of the horseshoe shape, the diagnostic performance of these criteria is inadequate. Diagnostic accuracy rates of 74% to 78% have been reported for the evaluation of lymph node metastasis by 4- to 64-row MDCT.[5, 8] Because microscopic infiltration cannot be assessed, the false-negative rate is approximately 10%. The false-positive rate has ranged from 3% to 43% due to reactive lymph node enlargement. An imaging finding other than enlargement is a low attenuation area resulting from central necrosis, and non-homogeneous contrast enhancement is a CT finding with a high positive predictive value.[14] If lymph node metastasis affects the clinical determination of a treatment plan, CT-guided biopsy/aspiration may be performed. Because the lung is the organ that is the most common site of distant RCC metastasis, chest CT is also performed. However, it has been reported that chest CT can be omitted in the absence of symptoms and abnormal test data in stages cT1a and cN0.[15]

2. MRI

MRI results in no radiation exposure and provides good tissue contrast. It is generally used when CT cannot be performed due to circumstances such as pregnancy or serious allergy to contrast media. MRI is useful when CT contrast enhancement is unevaluable, such as in the case of a hemorrhagic lesion. The diagnostic performance of MRI with respect to T staging and tumor thrombus has been reported to be roughly equal to that of 4-row MDCT.[2, 12] However, MDCT permits imaging to be performed over a wide

area in a short time, and it can be used to diagnose distant metastasis. Consequently, MRI has a limited role in staging.

A case in which MRI is useful is in assessing the feasibility of nephron-sparing surgery (differentiating T1a and T3a). Specifically, the combination of pseudocapsule rupture and changes in the peripheral fatty tissue in T2-weighted images yields high diagnostic performance (diagnostic accuracy rate, 91%) with respect to perirenal fat infiltration.[16] Moreover, MRI sequences such as true FISP are useful when assessing intravenous tumor thrombus is difficult with CT. MRI findings such as those concerned with embolus texture analysis and characteristics of the venous wall are useful for assessing venous wall invasion by tumor thrombus.[17, 18]

3. Bone scintigraphy

The reports to date have indicated that bone scintigraphy can be performed in circumstances where bone metastasis is strongly suspected, such as in the presence of bone pain. However, they indicate that it is of little value as a routine examination for staging.[19-23] In a retrospective study of 205 patients with pathologically demonstrated RCC, bone metastasis was present in 34 patients (17%), and sensitivity and specificity of 94% and 86%, respectively, were seen in an examination of the diagnostic performance of bone scintigraphy. However, its positive predictive value was a low 57%. Moreover, the bone metastasis rate in patients with stage T1-3aN0M0 disease and no bone pain was ≤ 5%. It was therefore concluded that bone scintigraphy is not recommended in such cases.[19]

Uchida et al. compared FDG-PET and bone scintigraphy in 227 patients with bone metastasis, including 21 patients with renal cancer. They reported that the lesion detection rate for osteolytic bone metastases was significantly lower with bone scintigraphy (19 lesions) than with FDG-PET (41 lesions).[24] In view of the fact that nearly all renal cancer bone metastases are osteolytic metastases, the sensitivity of bone scintigraphy cannot be considered high. Bone scintigraphy is not recommended as a routine examination for staging renal cancer. Its use is appropriate in patients for whom bone metastasis is strongly suspected, such as those in whom the degree of primary tumor progression is high and the likelihood of metastasis is also high and in those with bone pain or hematological abnormalities.

4. PET

PET (PET/CT) is currently covered by national health insurance in Japan for all malignancies except early gastric cancer if staging or the definitive diagnosis of metastasis and recurrence cannot be performed with another test or diagnostic imaging modality. In the case of renal cancer, an examination of the metastasis detection performance of FDG-PET/CT showed its sensitivity, specificity, and diagnostic accuracy rate to be 89.5%, 83.3%, and 85.7%, respectively, findings comparable to but not superior to those of conventional examinations.[25] Because of its advantages, however, it is recommended when diagnosis is difficult with conventional examinations. The advantages are the ability to perform whole-body screening with a single examination, and the fact that it can avoid renal dysfunction and allergy problems resulting

from the use of a contrast medium. FDG uptake in RCC is known to be low, and increased diagnostic accuracy is anticipated in the future with the use of other tracers instead of FDG.

Search keywords and secondary sources used as references

PubMed was searched using the following keywords: renal cell carcinoma, preoperative, staging, CT, MRI, bone scintigraphy, positron emission tomography, and chest CT.

In addition, the following were referenced as secondary sources.

1) Japanese Urological Association, Japanese Society of Pathology, and Japan Radiological Society, Ed.: The General Rule for Clinical and Pathological Studies on Renal Cell Carcinoma (5th Edition). Medical Review, 2020.
2) Japanese Urological Association, Ed.: 2017 Clinical Practice Guidelines for Renal Cancer. Medical Review, 2017.
3) Vikram R et al: ACR Appropriateness Criteria®: renal cell carcinoma staging. J Am Coll Radiol 13: 518-525, 2016

References

1) Kopka L et al: Dual-phase helical CT of the kidney: value of the corticomedullary and nephrographic phase for evaluation of renal lesions and preoperative staging of renal cell carcinoma. AJR Am J Roentogenol 169: 1573-1578, 1997
2) Hallscheidt PJ et al: Diagnostic accuracy of staging renal cell carcinomas using multidetector-row computed tomography and magnetic resonance imaging: a prospective study with histopathologic correlation. J Comput Assist Tomogr 28: 333-339, 2004
3) Roberts WW et al: Pathological stage does not alter the prognosis for renal lesions determined to be stage T1 by computerized tomography. J Urol 173: 713-715, 2005
4) Hallscheidt PJ et al: Multislice computed tomography in planning nephron-sparing surgery in a prospective study with 76 patients: comparison of radiological and histopathological findings in the infiltration of renal structures. J Comput Assist Tomogr 30: 869-874, 2006
5) Türkvatan A et al: Preoperative staging of renal cell carcinoma with multidetector CT. Diagn Interv Radiol 15: 22-30, 2009
6) Tsili AC et al: Perinephric fat invasion on renal cell carcinoma: evaluation with multidetector computed tomography-multivariate analysis. JCAT 36: 450-457, 2013
7) Hedgire SS et al: Preoperative evaluation of perinephric fat invasion in patients with renal cell carcinoma: correlation with pathological findings. Clinical Imaging 37: 91-96, 2013
8) Catalano C et al: High-resolution multidetector CT in the preoperative evaluation of patients with renal cell carcinoma. AJR Am J Roentgenol 180: 1271-1277, 2003
9) Bolster F et al: Renal cell carcinoma: accuracy of multidetector computed tomography in the assessment of renal sinus fat invasion. J Comput Assist Tomogr 40 (6): 851–855, 2016
10) Kim C et al: Diagnostic value of multidetector computed tomography for renal sinus fat invasion in renal cell carcinoma patients. Eur J Radiol 83: 914-918, 2014
11) Kresowik TP et al: Combined renal sinus fat and perinephric fat renal cell carcinoma invasion has a worse prognosis than either alone. J Urol 184: 48-52, 2010
12) Hallscheidt PJ et al: Preoperative staging of renal cell carcinoma with inferior vena cava thrombus using multidetector CT and MRI: prospective study with histopathological correlation. J Comput Assist Tomogr 29: 64-68, 2005
13) Guzzo TJ et al: The accuracy of multidetector computerized tomography for evaluating tumor thrombus in patients with renal cell carcinoma. J Urol 181: 486-460, 2009
14) Tsili AC et al: Advanced of multidetector computed tomography in the characterization and staging renal cell carcinoma. World J Radiol 7: 110-127, 2015.
15) Larcher A et al: When to perform preoperative chest computed tomography for renal cancer staging. BJU Int 20: 490-496, 2017
16) Roy C Sr et al: Significance of the pseudocapsule on MRI of renal neoplasms and its potential application for local staging: a retrospective study. AJR Am J Roentgenol 184: 113-120, 2005
17) Adams LC et al: Renal cell carcinoma with venous extension: prediction of inferior vena cava wall invasion by MRI. Cancer Imaging 18: 17, 2018
18) Alayed A et al: Diagnostic accuracy of MRI for detecting inferior vena cava wall invasion in renal cell carcinoma tumor thrombus using quantitative and subjective analysis. AJR Am J Roentgenol: 212: 562–569, 2019
19) Koga S et al: The diagnostic value of bone scan in patients with renal cell carcinoma. J Urol 166: 2126-2128, 2001

20) Rosen PR et al: Bone scintigraphy in the initial staging of patients with renal-cell carcinoma: concise communication. J Nucl Med 25: 289-291, 1984
21) Campbell RJ et al: Staging of renal cell carcinoma: cost-effectiveness of routine preoperative bone scans. Urology 25: 326-329, 1985
22) Blacher E et al: Value of routine radionuclide bone scans in renal cell carcinoma. Urology 26: 432-434, 1985
23) Staudenherz A et al: Is there a diagnostic role for bone scanning of patients with a high pretest probability for metastatic renal cell carcinoma? Cancer 85: 153-155, 1999
24) Uchida K et al: F-FDG PET/CT for diagnosis of osteosclerotic and osteolytic vertebral metastatic lesions: comparison with bone scintigraphy. Asian Spine J 7: 96-103, 2013
25) Park JW et al: Significance of 18F-fluorodeoxyglucose positron-emission tomography/computed tomography for the postoperative surveillance of advanced renal cell carcinoma. BJU Int 103: 615-619, 2009

BQ 71 Is CT recommended when a urothelial tumor of the upper urinary tract is suspected?

Statement

CT urography, which involves imaging in the excretory phase of contrast-enhanced CT, is recommended for patients in the high-risk group who are suspected of having an upper urinary tract urothelial tumor. The high-risk group includes patients with a history of urothelial tumors and middle-aged and elderly patients with macroscopic hematuria.

Background

The characteristics of urothelial carcinoma are multiple simultaneous occurrences and a high rate of recurrence. Its diagnosis requires detailed examination of the urinary tract as a whole, including the renal pelvis, ureter, and bladder. Although bladder tumors can be diagnosed by cystoscopy, upper urinary tract urothelial tumors are difficult to diagnose. CT urography is becoming widely used for the detailed examination of upper urinary tract tumors, and the evidence regarding its usefulness and issues is reviewed below.

Explanation

Intravenous urography has long been the first choice as an imaging modality for simple screening of the urinary tract as a whole, and CT urography using MDCT, which involves excretory phase imaging after contrast medium administration, has been reported to be useful. Maximum-intensity projection (MIP) or volume rendering (VR) enables intravenous urography-like pyelograms to be easily generated. CT urography also allows detailed observation of urinary tract and non-urinary tract lesions in normal high-resolution transverse images. In Europe and the United States, CT urography has rapidly become widely used, and intravenous urography is now rarely performed. The detection sensitivity of CT urography for upper urinary tract urothelial tumor has been reported to be very high, ranging from 91% to 97%.[1-3] An article that compared CT urography and intravenous urography with respect to the diagnostic results for upper urinary tract urothelial carcinoma in patients with hematuria reported sensitivity, specificity, and diagnostic accuracy of intravenous urography ranging from 75% to 80%, 81% to 86%, and 81% to 85%, respectively and those of CT urography ranging from 94% to 96%, 95% to 100%, and 94% to 99%, thus, the results for CT urography were superior to those for intravenous urography.[4, 5] The guidelines of the American College of Radiology give intravenous urography scores of 1, 2, and 3 points (the lowest rank out of 9 points) and CT urography scores of 7, 8, and 9 points (the highest rank) as a method for examining patients with hematuria (secondary source 1). The guidelines of the European Association of Urology and the Japanese Urological Association also strongly recommend CT urography to diagnose upper urinary tract tumors (secondary sources 2 and 3).

However, a problem with CT urography is that the radiation exposure involved in a single examination is 2 to 3 times higher than the radiation exposure with intravenous urography (~ 15 to 30 mSv with CT urography and 5 to 10 mSv with intravenous urography, according to previous reports). Consequently, the guidelines of the European Society of Urogenital Radiology recommend that the indication for CT urography be limited to patients aged ≥ 40 years with macroscopic hematuria, who are more likely to have urothelial carcinomas (secondary source 4). The use of the iterative reconstruction method and low-tube-voltage imaging is being widely implemented clinically to reduce the radiation exposure that has impeded widespread CT urography use.[6, 8] The use of low-tube-voltage imaging and dual-energy CT are also being widely adopted to reduce the contrast medium dose without reducing image quality. 8,9) In groups at high risk of upper urinary tract tumors, 3-phase imaging involving plain imaging, either corticomedullary- or nephrographic-phase imaging, and excretory phase imaging is generally performed, however, debate continues in this regard.[10]

Search keywords and secondary sources used as references

PubMed was searched using the following keywords: urothelial tumor, CT, and CT urography.

In addition, the following were referenced as secondary sources.

1) Wolfman DJ et al: ACR Appropriateness Criteria®: hematuria. J Am Coll Radiol 17: S138-S147, 2020
2) Rouprêt M et al: European Association of Urology guidelines on upper urinary tract urothelial carcinomas: 2020 update. Eur Urol 79 (1): 62-79, 2021
3) Oya M et al: Evidenced-based clinical practice guideline for upper tract urothelial carcinoma (summary--Japanese Urological Association, 2014 edition). Int J Urol 22 (1): 3-13, 2015 (replace this reference to English version identical to Japanese Guideline.
4) Van Der Molen AJ et al: CT urography: definition, indications and techniques: a guideline for clinical practice. Eur Radiol 18: 4-17, 2008

References

1) Cowan NC et al: Multidetector computed tomography urography for diagnosing upper urinary tract urothelial tumour. BJU International 99: 1363-1370, 2007
2) Chlapoutakis K et al: Performance of computed tomographic urography in diagnosis of upper urinary tract urothelial carcinoma, in patients presenting with hematuria: systematic review and meta-analysis. Eur J Radiol 73: 334-338, 2010
3) Wang LJ et al: Diagnostic accuracy of transitional cell carcinoma on multidetector computerized tomography urography in patients with gross hematuria. J Urol 181: 524-531, 2009
4) Wang LJ et al: Multidetector computerized tomography urography is more accurate than excretory urography for diagnosing transitional cell carcinoma of the upper urinary tract in adults with hematuria. J Urol 183: 48-55, 2010
5) Jinzaki M et al: Comparison of CT urography and excretory urography in the detection and localization of urothelial carcinoma of the upper urinary tract. AJR Am J Roentgenol 196: 1102-1109, 2011
6) Juri H et al: Low-dose computed tomographic urography using adaptive iterative dose reduction 3-dimensional: comparison with routine-dose computed tomography with filtered back projection. J Comput Assist Tomogr 37: 426-431, 2013
7) Kim SH et al: Comparison of full- and half-dose image reconstruction with filtered back projection or sinogram-affirmed iterative reconstruction in dual-source single-energy MDCT urography. AJR Am J Roentgenol 211: 641-648, 2018
8) Kim SY et al: Low-tube-voltage CT urography using low-concentration-iodine contrast media and iterative reconstruction: a multi-institutional randomized controlled trial for comparison with conventional CT urography. Korean J Radiol 19: 1119-1129, 2018
9) Shuman WP et al: Dual-energy CT urography with 50% reduced iodine dose versus single-energy CT urography with standard iodine dose. AJR Am J Roentgenol 212: 117-123, 2019
10) Fojecki G et al: Consultation on UTUC, Stockholm 2018 aspects of diagnosis of upper tract urothelial carcinoma. World J Urol 37: 22712278, 2019

BQ 72 Is MRI recommended to determine the invasion depth of bladder cancer?

Statement

MRI is recommended before transurethral resection of a bladder tumor if cystoscopy indicates possible muscle-invasive bladder cancer.

Background

In bladder cancer, the treatment plan and survival vary depending on invasion depth. The presence or absence of muscle invasion is particularly important for assessing the suitability of bladder-sparing treatment. Invasion depth determination that uses the high contrast resolution of MRI is considered reliable.

Explanation

Muscle invasion of bladder cancer is definitively determined by the pathological diagnosis of specimens resected in the transurethral resection of a bladder tumor (TUR-BT). However, underestimation is also known to occur not infrequently with pathological diagnosis.[1, 2)] MRI is normally omitted if small pedunculated lesions are observed by cystoscopy, and the likelihood of non-muscle invasive bladder cancer is high. MRI is performed for staging before TURBT for lesions for which muscle-invasive cancer cannot be ruled out by cystoscopy. The Vesical Imaging-Reporting and Data System (VI-RADS), which describes standard MRI imaging and diagnostic methods, was published in 2018 against a background of widespread MRI diagnosis of bladder cancer. The purpose of VI-RADS is to predict the muscle invasion of incipient or recurrent bladder cancer. MRI is performed before TURBT to avoid postoperative reactive change of the TURBT and to determine the VI-RADS morphological category. T2-weighted, diffusion-weighted, and dynamic contrast enhanced MRI are performed. Anatomical information is obtained with T2-weighted imaging. With diffusion-weighted and dynamic contrast imaging, contrast between tumors and normal tissue is high. Diffusion-weighted images and dynamic contrast-enhanced MRI play a central role in predicting muscle invasion. Prediction of the likelihood of muscle invasion is made according to the categorization table (Table). As the category number increases, the likelihood of muscle invasion increases. If the quality of the diffusion-weighted images is good, the category on diffusion-weighted imaging is adopted as the final determination. If the quality of the diffusion-weighted images is inadequate, the category on dynamic contrast imaging is adopted as the final determination. A meta-analysis found that, with the use of VI-RADS, sensitivity and specificity for muscle invasion were 0.83 (95% CI, 0.70 to 0.90) and 0.90 (95% CI, 0.83 to 0.95), respectively.[3)] Good interobserver agreement rates (kappa coefficients) ranging from 0.81 to 0.90 were reported. The reported prevalence of muscle-invasive cancer by category was 0% for category 1, 19% for category 2, 44% for category 3, 90% for category 4, and 94% for category 5 (investigation with 50% prevalence of muscle-invasive bladder cancer in all patients).[4)] At present, the

fact that the use of TURBT and pathological diagnosis is the general rule for diagnosing muscle invasion remains unchanged. However, MRI is expected to be a tool that complements their use. Moreover, the ability of CT to differentiate muscle-invasive cancer from non-muscle-invasive cancer is weak.

Table. Categories of the Vesical Imaging-Reporting and Data System (VI-RADS, prepared based on secondary source 2)

Category	T2-Weighted Imaging (structural category: SC)	Diffusion-Weighted Imaging (DW category)	Dynamic MRI (CE category)
1	Uninterrupted low SI line representing the integrity of muscularis propria (lesion <1 cm; exophytic tumor with or without stalk and/or thickened inner layer)	Muscularis propria with intermediate continuous SI on DWI (lesion <1 cm, hyperintense on DWI and hypointense on ADC, with or without stalk and/or low SI thickened inner layer on DWI)	No early enhancement of the muscularis propria (lesions corresponding to SC 1 findings)
2	Uninterrupted low SI line representing the integrity of muscularis propria (lesion >1 cm; exophytic tumor with stalk and/or high SI thickened inner layer, when present, or sessile/broad-based tumor with high SI thickened inner layer, when present)	Muscularis propria with continuous intermediate SI on DWI (lesion >1 cm, hyperintense on DWI and hypointense on ADC, with low SI stalk and/or low SI thickened inner layer on DWI, or broad-based/sessile tumor with low/intermediate SI thickened inner layer on DWI)	No early enhancement of muscularis propria with early enhancement of inner layer (lesions corresponding to SC 2 findings)
3	Lack of category 2 findings with associated presence of an exophytic tumor without stalk, or sessile/broad-based tumor without high SI thickened inner layer but with no clear disruption of low SI muscularis propria	Lack of category 2 findings (lesions corresponding to T2 category 3 findings) but with no clear disruption of low SI muscularis propria.	Lack of category 2 findings (lesions corresponding to SC category 3 findings) but with no clear disruption of low SI muscularis propria
4	Interruption of low SI line suggesting extension of the intermediate SI tumor tissue to muscularis propria	High SI tumor on DWI and low SI tumor on ADC extending focally to muscularis propria.	Tumor early enhancement extends focally to muscularis propria
5	Extension of intermediate SI tumor to extravesical fat, representing the invasion of the entire bladder wall and extravesical tissues	High SI tumor on DWI and low SI tumor on ADC extending to the entire bladder wall and extravesical fat.	Tumor early enhancement extends to the entire bladder wall and to extravesical fat

SI: signal intensity

Panebianco V et al: Multiparametric magnetic resonance imaging for bladder cancer: development of VI-RADS (Vesical Imaging-Reporting And Data System). Eur Urol 74: 294-306, 2018

Search keywords and secondary sources used as references

PubMed was searched using the following keywords: magnetic resonance imaging, urinary bladder neoplasms, and neoplasm staging.

In addition, the following were referenced as secondary sources.

1) Japanese Urological Association, Ed.: 2019 Clinical Practice Guidelines for Bladder Cancer. Igakutosho Shuppan, 2019.
2) Panebianco V et al: Multiparametric magnetic resonance imaging for bladder cancer: development of VI-RADS (Vesical Imaging-Reporting And Data System). Eur Urol 74: 294-306, 2018

References

1) Cumberbatch MGK et al: Repeat transurethral resection in non-muscle-invasive bladder cancer: a systematic review. Eur Urol 73: 925-933, 2018
2) Naselli A et al: Role of restaging transurethral resection for T1 non-muscle invasive bladder cancer: a systematic review and meta-analysis. Eur Urol Focus 4: 558-567, 2018
3) Woo S et al: Diagnostic performance of vesical imaging reporting and data system for the prediction of muscle-invasive bladder cancer: a systematic review and meta-analysis. Eur Urol Oncol 3: 306-315, 2020
4) Ueno Y et al: Diagnostic accuracy and interobserver agreement for the Vesical Imaging-Reporting and Data System for muscle-invasive bladder cancer: a multireader validation study. Eur Urol 76: 54-56, 2019

CQ 17 Is omitting contrast-enhanced MRI recommended when MRI is performed to detect clinically significant prostate cancer in patients with incipient disease?

Recommendation

Omitting contrast-enhanced MRI is weakly recommended for MRI examinations performed to detect clinically significant prostate cancer. This applies only to facilities capable of all of the following: 3T-MRI imaging under appropriate conditions, image evaluation by a radiologist with extensive experience interpreting prostate MRI, and pathological diagnosis by biopsy guided by location information obtained with MRI.

Recommendation strength: 2, strength of evidence: weak (C), agreement rate: 87% (13/15)

Background

Prostate cancer is a malignancy that affects approximately 90,000 people in Japan. It is classified as either clinically significant (CS) cancer that requires therapeutic intervention or clinically insignificant/not clinically significant (NCS) cancer with little need for intervention. There have been numerous recent reports that prostate MRI can efficiently detect CS cancer, and its role as a pre-biopsy examination has come to be regarded as important. The initial version of the Prostate Imaging Reporting and Data System (PI-RADS), which describes standard MRI examination and diagnostic methods for prostate cancer, indicated that it is diagnosed by multiparametric MRI (mpMRI), which combines T2-weighted, diffusion-weighted, and dynamic contrast-enhanced imaging (secondary source 1). Beginning from version 2, however, PI-RADS has indicated that the role of dynamic contrast-enhanced imaging is limited (secondary sources 2 and 3). Since then, there has been increased reporting of the usefulness of biparametric MRI (bpMRI), which omits dynamic contrast-enhanced imaging and uses only T2-weighted and diffusion-weighted imaging. Because bpMRI does not involve the use of a contrast medium, reductions in examination time and cost and a decrease in the workload of medical staff can be expected, and there is no need for concern about adverse reactions to a contrast medium. On the other hand, there is apprehension about lower detection performance with bpMRI than with mpMRI in CS cancers.

For the present discussion, the question of whether omitting contrast-enhanced MRI is recommended when MRI examination is performed to detect incipient CS cancer was raised as a CQ, and a qualitative systematic review was conducted regarding bpMRI and mpMRI.

Explanation

For this systematic review, a decrease in CS cancer detection performance was specified as an adverse outcome. A literature search for studies that compared the diagnostic performance of bpMRI and mpMRI was performed using the keywords indicated below and yielded 9 relevant articles.[1-9)] All 9 articles were reports of cross-sectional studies. In all but 1 of the articles on MRI, 3T systems were used. In all of the articles, the image evaluations were performed by radiologists with abundant experience in interpreting prostate MRI. For the MRI evaluation method, criteria basically in accordance with PI-RADS or original diagnostic criteria such as a Likert scale were adopted. In nearly all of the articles, pathological diagnosis involved either total prostatectomy or targeted biopsy guided by location information obtained with MRI. Although there is no internationally uniform definition of CS cancer, the definition used in the 9 articles was similar to that adopted clinically (Table). The 9 articles had a low risk of bias and low indirectness.

The sensitivity, specificity, and diagnostic accuracy rate for CS cancer ranged from 53% to 96%, 15% to 93%, and 42% to 89%, respectively, with bpMRI and from 52% to 95%, 16% to 93%, and 42% to 88% for mpMRI. Thus, the diagnostic performance of bpMRI and mpMRI was roughly equal.[1-9)] In 3 articles, an ROC analysis was performed. AUC ranged from 0.68 to 0.81 with bpMRI and from 0.71 to 0.79 with mpMRI. Thus, no difference was seen between the 2 methods.[2, 4, 7)] One article that used a PI-RADS (version 2) category of 4 or higher as the criterion for a positive finding reported a trade-off between sensitivity and specificity, with significantly lower sensitivity (63% vs. 80%) and significantly higher specificity (72% to 45%) seen with bpMRI than with mpMRI. Thus, the results showed that the number of false-negative lesions increased if a contrast medium was not used (adverse outcome).[2)] However, the diagnostic accuracy rate (66% vs. 71%) and AUC (0.81 vs. 0.79) were similar for the 2 methods.[2)]

Table. Definition of clinically significant prostate cancer used in the 9 articles extracted in the systematic review

Definition	Reference No.
Lesion with GS ≥ 7	1), 3), 9)
Lesion with GS ≥ 7 and/or tumor volume ≥ 0.5 mL and/or lesion with extracapsular extension	2)
Lesion with GS ≥ 7 and/or lesion with extracapsular extension	4)
Lesion with GS ≥ 7 and/or lesion with tumor length ≥ 5 mm	5)
Lesion with intermediate to high risk (NCCN guidelines*)	6)
Lesion with GS ≥ 7 and/or lesion with tumor volume ≥ 5 mL	7)
GS 6 lesion with more than 3 positive cores by biopsy and/or GS 6 lesion that occupies ≥ 50% of biopsy length or lesion with GS ≥ 7	8)

GS: Gleason score, NCCN: National Comprehensive Cancer Network

* Prostate cancer risk classification from NCCN guidelines (version 2.2014)
low risk: PSA (prostate specific antigen) ≤ 10 ng/mL, GS ≤ 6, and T1-T2a
intermediate risk: PSA=10-20 ng/mL, GS 7, and T2b
high risk: PSA > 20 ng/mL, and/or GS ≥ 8, and/or T2c-T3a

Based on the above findings, the conclusion of this systematic review was that bpMRI and mpMRI are comparable in diagnostic performance.

Although no systematic review was conducted for measures other than diagnostic performance, it is self-evident that omitting contrast-enhanced MRI shortens the examination time, reduces the cost burden, and eliminates the risk of contrast medium adverse reactions for the patient. For medical staff, it eliminates the need to interview the patient about contrast media, secure a route for contrast medium administration, and address adverse reactions. It also shortens the length of imaging performed by the radiological technologist, reducing the workload of medical staff. A bpMRI examination that omits contrast-enhanced MRI is therefore weakly recommended to detect CS cancer. This applies only to facilities capable of all of the following: 3T-MRI imaging under appropriate conditions, image evaluation by a radiologist with extensive experience interpreting prostate MRI, and pathological diagnosis by biopsy guided by location information obtained with MRI. Conversely, evaluation by mpMRI that includes contrast-enhanced MRI is preferable at facilities that cannot meet the above preconditions. This is due to concern about lower detection performance with bpMRI than with mpMRI in CS cancer. In performing bpMRI examinations, hyoscine butylbromide needs to be administered before the examination to reduce motion artifacts caused by gastrointestinal peristalsis. In addition, imaging acquisition techniques that are in accordance with PI-RADS should be determined, such as high-spatial-resolution T2-weighted imaging and high b-value (≥ 1,400 s/mm^2) diffusion-weighted imaging (secondary sources 2 and 3). Moreover, because the subjects assessed in this systematic review were patients with clinically suspected CS cancer, these recommendations do not apply to prostate cancer screening. They also do not apply to patients with a higher than normal risk for prostate cancer, such as those with a family history of prostate cancer and those with prior negative biopsy and elevated PSA levels, due to concern about the major detriment that would result from a bpMRI false-negative. In addition, the diagnostic performance of bpMRI and mpMRI for detecting post-treatment recurrent tumors and staging (extracapsular extension, seminal vesicle invasion) has not been shown to be comparable, and contrast-enhanced examinations are therefore added as needed.

Search keywords and secondary sources used as references

PubMed was searched using the following keywords: prostate neoplasms, prostate cancer, clinically significant cancer, magnetic resonance imaging, multiparametric MRI, biparametric MRI, abbreviated MRI, and Prostate Imaging Reporting and Data System (PI-RADS).

In addition, the following were referenced as secondary sources.

1) Barentsz JO et al: ESUR prostate MR guidelines 2012. Eur Radiol 22: 746-757, 2012
2) Weinreb JC et al: PI-RADS Prostate Imaging - Reporting and Data System 2015, Version 2. Eur Urol 69: 16-40, 2016
3) Turkbey B et al: Prostate Imaging Reporting and Data System Version 2.1: 2019 Update of Prostate Imaging Reporting and Data System Version 2. Eur Urol 76: 340-351, 2019

References

1) van der Leest M et al: High diagnostic performance of short magnetic resonance imaging protocols for prostate cancer detection in biopsy-naive men: the next step in magnetic resonance imaging accessibility. Eur Urol 76: 574-581, 2019
2) Choi MH et al: Prebiopsy biparametric MRI for clinically significant prostate cancer detection with PI-RADS version 2: a multicenter study. AJR Am J Roentgenol 212: 839-846, 2019
3) Mussi TC, et al: Comparison between multiparametric MRI with and without post - contrast sequences for clinically significant prostate cancer detection. Int Braz J Urol 44: 1129-1138, 2018
4) Di Campli E et al: Diagnostic accuracy of biparametric vs multiparametric MRI in clinically significant prostate cancer: comparison between readers with different experience. Eur J Radiol 101: 17-23, 2018
5) Lee DH et al: Comparison of multiparametric and biparametric MRI in first round cognitive targeted prostate biopsy in patients with PSA levels under 10 ng/mL. Yonsei Med J 58: 994-999, 2017
6) Kuhl CK et al: Abbreviated biparametric prostate MR imaging in men with elevated prostate-specific antigen. Radiology 285: 493-505, 2017
7) Barth BK et al: Detection of clinically significant prostate cancer: short dual-pulse sequence versus standard multiparametric MR imaging: a multireader study. Radiology 284: 725-736, 2017
8) Mussi TC et al: Are dynamic contrast-enhanced images necessary for prostate cancer detection on multiparametric magnetic resonance imaging? Clin Genitourin Cancer 15: e447-e454, 2017
9) Thestrup KC et al: Biparametric versus multiparametric MRI in the diagnosis of prostate cancer. Acta Radiol Open 5: 2058460116663046, 2016

BQ 73 Is MRI recommended for the local staging of prostate cancer?

Statement

MRI is recommended to evaluate extracapsular and seminal vesicle invasion in prostate cancer of intermediate or high risk.

(Note: With a body surface coil, a ≥ 1.5T system needs to be used, and the imaging conditions must be optimized.)

Background

Prostate cancer is increasing, making it important to standardize the diagnostic imaging methods. Although MRI is considered a reliable diagnostic imaging method for the local staging of prostate cancer, it is not performed for all patients. Whether MRI is useful for the local staging of prostate cancer (extracapsular invasion, seminal vesicle invasion) and the circumstances in which its usefulness increases are examined below.

Explanation

MRI is considered the most reliable diagnostic imaging method for the local staging of prostate cancer. The Prostate Imaging and Reporting and Data System (PI-RADS) has been widely adopted in recent years to decrease the variability in MRI diagnostic performance that occurs depending on the experience of the reader and to standardize imaging and interpretation methods. However, its main objective is cancer detection, and a specific scoring method for local staging has not been established (secondary source 2). Many investigations that have examined MRI diagnostic performance with respect to extracapsular extension have used transrectal coils. Recently, however, more investigations have used a 3T-MRI system without using a transrectal coil. High-resolution T2-weighted imaging is necessary to accurately evaluate extracapsular extension and neurovascular bundle and seminal vesicle invasion. However, a 3T-MRI system is advantageous because it enables thin-slice, high-spatial-resolution imaging to be performed using a body surface coil.

Reliable T2-weighted imaging findings for extracapsular extension include the following: ① changes in the prostate contour (local protrusion and asymmetry), ② morphological changes in the adjacent neurovascular bundles (left-right asymmetry), ③ rupture of the capsular structure, ④ obliteration of rectoprostatic angle, and ⑤ direct invasion to the neurovascular bundles. These findings are not all given the same weight. Findings ① and ② are indirect findings, whereas ④ and ⑤, which directly indicate an extraprostatic mass, are more strongly suggestive of extracapsular extension. Finding ⑥, the tumor contact length with the prostatic capsule, has been designated a predictor of extracapsular invasion. A contact length of ≥ 6 mm is suggestive of slight extracapsular invasion, and a contact length of ≥ 10 mm is suggestive of unambiguous extracapsular invasion.[1)] Reports vary regarding the diagnostic performance of

T2-weighted imaging with respect to extracapsular extension. Sensitivity, specificity, and diagnostic accuracy have been found to range from 22% to 82%, 70% to 100%, and 61% to 84%, respectively.[2-17] In a meta-analysis by de Rooij et al. that compiled data on the diagnostic performance of MRI in staging, the pooled sensitivity and specificity for extracapsular extension were 57% (95% CI, 49% to 64%) and 91% (95% CI, 88% to 93%), respectively.[18] Diagnostic performance is also determined by whether the evaluation can be performed in the plane orthogonal to the surface where the tumor and capsule are in contact.

Although T2-weighted imaging plays the central role in evaluating extracapsular extension, the certainty of extracapsular extension is increased by the addition of diffusion-weighted imaging.[19] However, whether adding an evaluation of extracapsular extension by dynamic contrast imaging to T2-weighted imaging is meaningful depends, in part, on the experience of the reader.[13, 20]

Findings in T2-weighted images for seminal vesicle invasion include the localized or diffuse elimination of the botryoidal internal structure of the seminal vesicle due to a hypointense mass, localized thickening of the seminal vesicle wall and septum, and elimination of the angle between the prostate and seminal vesicle.[21] Reports on diagnostic performance with respect to seminal vesicle invasion have indicated sensitivity, specificity, and diagnostic accuracy ranging from 23% to 100%, 75% to 100%, and 76% to 97%, respectively.[3-6, 8-10, 14-17] A meta-analysis regarding seminal vesicle invasion showed sensitivity of 51% without the use of a transrectal coil and 59% with transrectal coil use for T2-weighted imaging.[18] With the addition of diffusion-weighted or dynamic contrast imaging, sensitivity increased from 53% to 64%.[18]

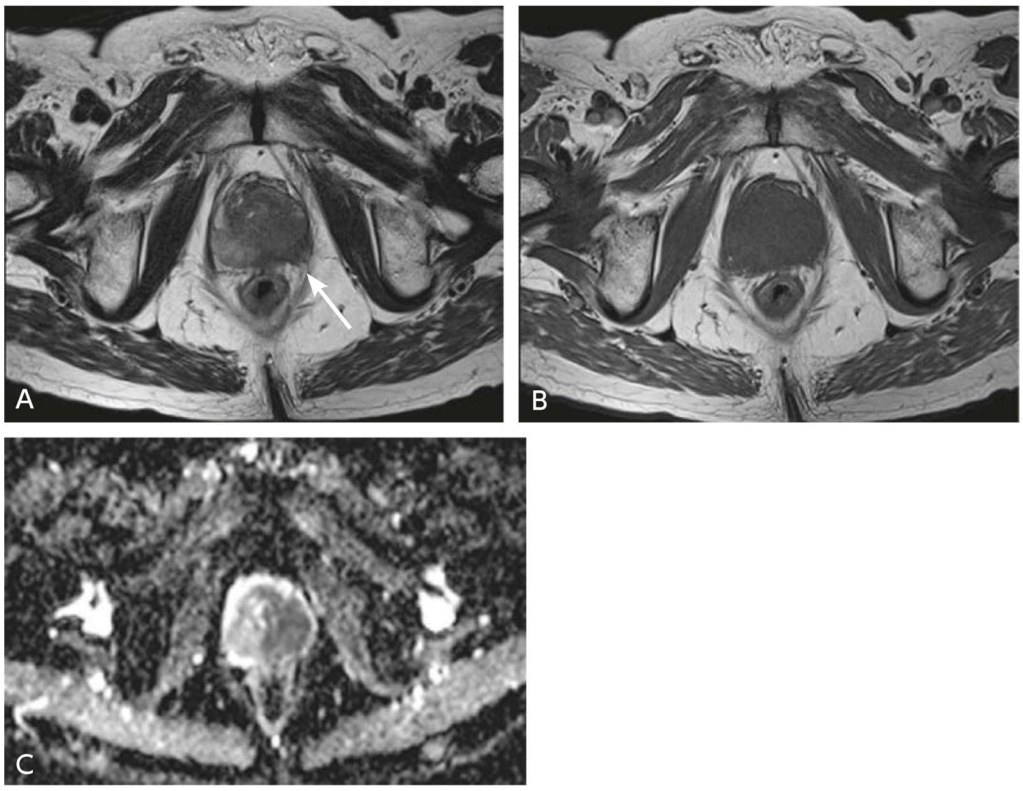

Figure. Prostate cancer (patient with PSA of 22 ng/mL)

A: MRI, T2-weighted image; B: MRI, T1-weighted image; C: MRI, ADC map, b-value = 1,000 s/mm^2
The left border area has changed to hypointense in the T2-weighted image, and this extends to the transitional area. Cancer is therefore suspected. The contour of the left dorsal region is spiny and shows a signal similar to that of the main lesion. Extracapsular invasion is suspected (→). The T1-weighted image clearly shows the disturbance of the contour. The ADC map clearly shows the intraprostatic tumor distribution, but it cannot indicate extracapsular progression in detail.

In the diagnosis and treatment of prostate cancer, appropriate treatment is selected by taking into account the risk classification, which combines the clinical stage, prostate-specific antigen (PSA) level, Gleason score, and the amount of cancer tissue in the biopsy needle. In Europe and the United States, it is also widely recognized that, when an imaging examination is performed, the examination is selected by taking into account the risk of the tumor. This is also indicated in guidelines [European Association of Urology (EAU) 2020, secondary source 3; American College of Radiology (ACR) 2017, secondary source 4]. A retrospective investigation found that MRI diagnostic performance with respect to extraprostatic extension was poor in low-risk patients, but good in patients at moderate or greater risk. However, the variation in specificity between risk levels was small.[8)] Patients with a PSA level > 10 mg/mL or Gleason score > 7 on biopsy are considered to be at moderate or greater risk, and evaluating extracapsular and seminal vesicle invasion by MRI has merit in such cases.

In Japan, diagnosis is often performed by imaging using a body surface coil, such as a pelvic phased-array coil. Imaging with an integrated system that uses both a body surface coil and a transrectal coil improves staging compared with imaging using a body surface coil alone.[14)] However, transrectal coil

use has not been widely adopted in Japan. Even if only a body surface coil is used, no large difference in staging capability is seen if a ≥ 1.5T MRI system is used and imaging is performed after the elimination of rectal gas, which reduces image quality, with a thin slice thickness of approximately 4 mm and good spatial resolution.[17] The most recent version of PI-RADS, version 2.1, indicates that the use of a transrectal coil is not required (secondary source 2).

Multiparametric MRI combines T2-weighted imaging, which has customarily been used to show morphological images, with functional imaging methods such as diffusion-weighted imaging or dynamic contrast imaging. Although its impact does not extend to cancer detection, mpMRI may improve pretreatment staging by incorporating information such as clinical data, tumor volume, and the length of the area of contact between a tumor and the prostatic capsule.[11, 22-24]

Search keywords and secondary sources used as references

PubMed was searched using the following keywords: prostate cancer, staging, and MRI.

In addition, the following were referenced as secondary sources.

1) Japan Radiological Society, Ed.: Diagnostic Imaging Guidelines 2016. KANEHARA & Co., 2016.
2) Turkbey B et al: Prostate Imaging Reporting and Data System Version 2.1: 2019 update of Prostate Imaging Reporting and Data System Version 2. Eur Urol 76: 340-351, 2019
3) Mottet N et al: EAU guidelines on prostate cancer. European Association of Urology, 2020
4) Coakley FV et al: ACR Appropriateness Criteria®: prostate cancer-pretreatment detection, surveillance, and staging. J Am Coll Radiol 14: S245-S257, 2017

References

1) Rosenkrantz AB et al: Length of capsular contact for diagnosing extraprostatic extension on prostate MRI: assessment at an optimal threshold. J Magn Reson Imaging 43: 990-997, 2016
2) Yu KK et al: Detection of extracapsular extension of prostate carcinoma with endorectal and phased-array coil MR imaging: multivariate feature analysis. Radiology 202: 697-702, 1997
3) Sanchez-Chapado M et al: Comparison of digital rectal examination, transrectal ultrasonography, and multicoil magnetic resonance imaging for preoperative evaluation of prostate cancer. Eur Urol 32: 140-149, 1997
4) Presti JC Jr et al: Local staging of prostatic carcinoma: comparison of transrectal sonography and endorectal MR imaging. Am J Roentgenol 166: 103-108, 1996
5) Cornud F et al: Local staging of prostate cancer by endorectal MRI using fast spin-echo sequences: prospective correlation with pathological findings after radical prostatectomy. Br J Urol 77: 843-850, 1996
6) Perrotti M et al: Endo-rectal coil magnetic resonance imaging in clinically localized prostate cancer: is it accurate? J Urol 156: 106-109, 1996
7) Ogura K et al: Dynamic endorectal magnetic resonance imaging for local staging and detection of neurovascular bundle involvement of prostate cancer: correlation with histopathologic results. Urology 57: 721-726, 2001
8) Allen DJ et al: Does body-coil magnetic-resonance imaging have a role in the preoperative staging of patients with clinically localized prostate cancer? BJU Int 94: 534-538, 2004
9) Nakashima J et al: Endorectal MRI for prediction of tumor site, tumor size, and local extension of prostate cancer. Urology 64: 101-105, 2004
10) Chelsky MJ et al: Use of endorectal surface coil magnetic resonance imaging for local staging of prostate cancer. J Urol: 150: 391-395, 1993
11) Wang L et al: Prostate cancer: incremental value of endorectal MR imaging findings for prediction of extracapsular extension. Radiology 232: 133-139, 2004
12) Brassell SA et al: Correlation of endorectal coil magnetic resonance imaging of the prostate with pathologic stage. World J Urol 22: 289-292, 2004

13) Fütterer JJ et al: Staging prostate cancer with dynamic contrast-enhanced endorectal MR imaging prior to radical prostatectomy: experienced versus less experienced readers. Radiology 237: 541-549, 2005
14) Fütterer JJ et al: Prostate cancer: comparison of local staging accuracy of pelvic phased-array coil alone versus integrated endorectal–pelvic phased-array coils. Local staging accuracy of prostate cancer using endorectal coil MR imaging. Eur Radiol 17: 1055-1065, 2007
15) Chandra RV et al: Endorectal magnetic resonance imaging staging of prostate cancer. ANZ J Surg 77: 860-865, 2007
16) Park BK et al: Comparison of phased-array 3.0-T and endorectal 1.5-T magnetic resonance imaging in the evaluation of local staging accuracy for prostate cancer. J Comput Assist Tomogr 31: 534-538, 2007
17) Lee SH et al: Is endorectal coil necessary for the staging of clinically localized prostate cancer?: comparison of non-endorectal versus endorectal MR imaging. World J Urol 28: 667-672, 2010
18) de Rooij M et al: Accuracy of magnetic resonance imaging for local staging of prostate cancer: a diagnostic meta-analysis. Eur Urol 70: 233-245, 2016
19) Woo S et al: Extracapsular extension in prostate cancer: added value of diffusion-weighted MRI in patients with equivocal findings on T2-weighted imaging. AJR Am J Roentgenol 204: W168-175, 2015
20) Bloch BN et al: Prediction of prostate cancer extracapsular extension with high spatial resolution dynamic contrast-enhanced 3-T MRI. Eur Radiol 22: 2201–2210, 2012.
21) Roethke M et al: Seminal vesicle invasion: accuracy and analysis of infiltration patterns with high-spatial resolution T2-weighted sequences on endorectal magnetic resonance imaging. Urol Int 92: 294-299, 2014
22) Schieda N et al: MRI assessment of pathological stage and surgical margins in anterior prostate cancer (APC) using subjective and quantitative analysis. J Magn Reson Imaging 45: 1296-1303, 2017
23) Lim C et al: Evaluation of apparent diffusion coefficient and MR volumetry as independent associative factors for extra-prostatic extension (EPE) in prostatic carcinoma. J Magn Reson Imaging 43: 726-736, 2016
24) Baco E et al: Predictive value of magnetic resonance imaging determined tumor contact length for extracapsular extension of prostate cancer. J Urol 193: 466, 2015

BQ 74 Is bone scintigraphy recommended for prostate cancer staging and posttreatment follow-up?

Statement

The use of bone scintigraphy should be avoided in low-risk patients (PSA ≤ 10 ng/mL, Gleason score ≤ 7) because of the low positivity rate. However, it is useful in patients with symptoms suggestive of bone metastasis and posttreatment PSA-recurrent patients.

Background

Following the lymph nodes, bone is the second most common organ for prostate cancer metastasis. Bone scintigraphy is a nuclear medicine examination that uses a ^{99m}Tc-labeled phosphate compound (methylene diphosphonate, hydroxymethylene diphosphonate). Its benefit is that it enables sensitive whole-body screening for bone lesions. Although it has long been used in prostate cancer care, the routine use of bone scintigraphy for staging and posttreatment follow-up poses problems from the perspectives of radiation exposure and cost. Recently, computer-aided diagnosis (CAD) has been introduced to bone scintigraphy, and there have been sporadic reports indicating that it is useful for improving diagnostic performance and predicting prognosis. This section reviews the relatively recent literature dealing with bone scintigraphy in prostate cancer and summarizes how it is used.

Explanation

In a meta-analysis that compared the diagnostic performance of choline-PET/CT (not covered by national health insurance in Japan), MRI, and bone scintigraphy with respect to bone metastasis in prostate cancer, an analysis of 11 articles on a per-patient basis showed that the sensitivity and specificity of bone scintigraphy were 79% and 82%, respectively, and that the diagnostic performance of bone scintigraphy was inferior to that of choline-PET/CT and MRI.[1)]

Rather than diagnostic performance, many recent studies of bone scintigraphy in prostate cancer have examined the positivity rate of bone scintigraphy according to patient characteristics (e.g., serum PSA level, Gleason score, T stage of the primary tumor).[2-9)] A position that reflects these observations and is common to the guidelines of urology societies in Japan, Europe, and the United States is that patients with a PSA level of ≤ 10 ng/mL and Gleason score ≤ 7 who are asymptomatic are at low risk of metastasis, and that bone scintigraphy for staging is not recommended for such patients. However, it may be meaningful for identifying lesion locations in patients such as those with symptoms suggestive of bone lesions and posttreatment PSA-recurrent patients (particularly patients with a high PSA doubling rate). Several reports describe improved diagnostic performance with respect to bone metastasis when SPECT or SPECT/CT is added to bone scintigraphy.[10-12)] However, the prolonged imaging duration and, in the case of SPECT/CT, CT radiation exposure, pose problems for these methods. Rather than being routinely added, SPECT or

SPECT/CT imaging should be performed when findings difficult to assess by planar imaging are obtained, and the imaging should be restricted to a localized area.

With regard to the diagnostic performance of CAD, many articles indicate that its sensitivity and specificity both exceed 80%.[13-15] It should be noted, however, that CAD basically just separates lesions according to the likelihood that they are benign or malignant based on pattern recognition, and it in no way reflects factors such as patient characteristics and findings from other imaging examinations. The bone scan index (BSI), which uses CAD to quantify the degree of whole-body abnormal bone uptake, has been reported to be an index that predicts treatment efficacy and an independent prognosis predictor (reflecting patient prognosis).[16,17] BSI is an objective index of posttreatment decreased uptake, and it is considered particularly useful for evaluating the condition of certain patients, such as those with diffuse bone metastases.

Search keywords and secondary sources used as references

PubMed was used to search the literature with the following keywords: prostate cancer, bone metastasis, bone scan, and bone scintigraphy. The period searched was from 2015 to June 2019, and 1 new article (reference 17) was used in the review. Consequently, including the 16 articles cited in the 2016 edition of the guidelines (CQ147), a total of 17 articles were cited.

In addition, the following were referenced as secondary sources.

1) Japanese Urological Association, Ed.: 2016 Clinical Practice Guidelines for Prostate Cancer. Medical Review, 2016.
2) Mottet N et al: EAU guidelines on prostate cancer. European Association Urology, 2020

References

1) Shen G et al: Comparison of choline-PET/CT, MRI, SPECT, and bone scintigraphy in the diagnosis of bone metastases in patients with prostate cancer: a meta-analysis. Skeletal Radiol 43: 1503-1513, 2014
2) Zacho HD et al: Prospective multicenter study of bone scintigraphy in consecutive patients with newly diagnosed prostate cancer. Clin Nucl Med 39: 26-31, 2014
3) Tanaka N et al: Bone scan can be spared in asymptomatic prostate cancer patients with PSA of ≤ 20 ng/ml and Gleason score of ≤ 6 at the initial stage of diagnosis. Jpn J Clin Oncol 41: 1209-1213, 2011
4) Lee SH et al: Is it suitable to eliminate bone scan for prostate cancer patients with PSA ≤ 20 ng/ml? World J Urol 30: 265- 269, 2012
5) Palvolgyi R et al: Bone scan overuse in staging of prostate cancer: an analysis of a veterans affairs cohort. Urology 77: 1330-1337, 2011
6) Briganti A et al: When to perform bone scan in patients with newly diagnosed prostate cancer: external validation of the currently available guidelines and proposal of a novel risk stratification tool. Eur Urol 57: 551-558, 2010
7) Hirobe M et al: Bone scanning: who needs it among patients with newly diagnosed prostate cancer? Jpn J Clin Oncol 37: 788-792, 2007
8) Ishizuka O et al: Prostate-specific antigen, Gleason sum and clinical T stage for predicting the need for radionuclide bone scan for prostate cancer patients in Japan. Int J Urol 12: 728-732, 2005
9) Yap BK et al: Are serial bone scan useful for the follow-up of clinically localized, low to intermediate grade prostate cancer managed with watchful observation alone? BJU Int 91: 613-617, 2003
10) McLoughlin LC et al: The improved accuracy of planar bone scintigraphy by adding single photon emission computed tomography (SPECT-CT) to detect skeletal metastases from prostate cancer. Ir J Med Sci 185: 101-105, 2016
11) Helyar V et al: The added value of multislice SPECT/CT in patients with equivocal bony metastasis from carcinoma of the prostate. Eur J Nucl Med Mol Imaging 37: 706-713, 2010
12) Even-Sapir E et al: The detection of bone metastases in patients with high-risk prostate cancer: ^{99m}Tc-MDP planar bone scintigraphy, single- and multi-field-of-view SPECT, ^{18}F-fluoride PET, and ^{18}F-fluoride PET/CT. J Nucl Med 47: 287-297, 2006

13) Koizumi M et al: Evaluation of a computer-assisted diagnosis system, BONENAVI version 2, for bone scintigraphy in cancer patients in a routine clinical setting. Ann Nucl Med 29: 138-148, 2015
14) Takahashi Y et al: Assessment of bone scans in advanced prostate carcinoma using fully automated and semi-automated bone scan index methods. Ann Nucl Med 26: 586-593, 2012
15) Sadik M et al: Improved classification of planar whole-body bone scans using a computer-assisted diagnosis system: a multicenter, multiple-reader, multiple-case study. J Nucl Med 50: 368-375, 2009
16) Mitsui Y et al: Prediction of survival benefit using an automated bone scan index in patients with castration-resistant prostate cancer. BJU Int 110: E628-E634, 2012
17) Zacho HD et al: Bone scan index is an independent predictor of time to castration-resistant prostate cancer in newly diagnosed prostate cancer: a prospective study. Urology 108: 135-141, 2017

BQ 75 Which imaging examinations are recommended for staging testicular tumors?

Statement

There is strong evidence that CT is useful for this purpose, and it is therefore recommended. There is no adequate scientific basis for recommending PET.

Background

Because most testicular tumors are testicular germ cell tumors, where simply “testicular tumors” is used below it refers to testicular germ cell tumors. With recent advances in chemotherapy, the cure rate for testicular tumors has become very high. According to a 2006 report, the 5-year survival rate was 94% for the good-risk group based on the classification of the International Germ Cell Cancer Collaborative Group, 83% for the intermediate-risk group, and 71% for the poor-risk group.[1)] One of the most important factors in achieving a high cure rate is accurate staging. The staging classification of the Japanese Urological Association is determined by the location and size of metastases. Based on these considerations, imaging examinations for staging testicular tumor—specifically CT and PET—were examined.

Explanation

CT is an examination that is necessary for staging testicular tumors. It is strongly recommended for this purpose in the representative guidelines for Europe and the United States, such as those of the American College of Radiology (ACR) and European Association of Urology (EAU), as well as the Japanese Urological Association (secondary sources 1 to 3). The most frequent sites of testicular tumor metastases are the retroperitoneal lymph nodes. Therefore, the entire abdomen should always be scanned. Although the diagnosis of retroperitoneal lymph node metastasis by CT (Fig.) basically involves the use of size criteria, sensitivity and specificity largely depend on the cutoff value used. Hilton et al. reported that when a cutoff of 10 mm was used, specificity was 100%, but sensitivity was only 37%.[2)] Lowering this to 4 mm improved sensitivity to 93%, but specificity was 58%. To strike a balance between sensitivity and specificity, Hudolin et al. proposed a cutoff of 7 to 8 mm.[3)] Moreover, lymph node length in the craniocaudal direction has been found to be correlated with metastasis,[4)] and MPR in coronal as well as transverse imaging planes, is useful. Diagnosis based on size has limitations, such as the fact that changes such as inflammatory swelling result in false positives, in addition to the fact that small metastases result in false negatives. However, diagnostic performance can be improved to some extent by understanding lymph flow anatomy. That is, with a right testicular tumor, the primary landing zone is the infrarenal inter-aortocaval lymph nodes, followed by the paracaval, the precaval, and preaortic lymph nodes. With a left testicular tumor, on the other hand, the primary landing zone is the infrarenal paraaortic lymph nodes, followed by the inter-aortocaval and the preaortic lymph nodes. Particular attention is needed if the lymph nodes at these sites are conspicuous.

For pulmonary metastasis detection, chest CT is more sensitive than plain chest radiography. However, it often produces false positives for lung lesions ≤ 10 mm in size. With stage I seminomas, it may be possible to omit chest CT if there are no abnormalities on chest radiography.[5)] Chest CT is considered excellent for detecting mediastinal lymph node metastasis, although there have been few reports in this regard.

No firm conclusion has been reached regarding the usefulness of adding FDG-PET for staging. PET performed to stage nonseminomas has been reported to provide significantly better sensitivity and negative predictive value than CT.[6, 7)] However, a 2007 prospective, multicenter study examined 111 patients who were positive for stage I vascular invasive nonseminomas. Of these, 87 were found to be negative by PET and underwent follow-up without treatment. During a median follow-up period of 12 months, recurrence was seen in 33 of these 87 patients, and the study was terminated early. Moreover, 37% had a recurrence within 1 year. These findings indicate non-treatment follow-up cannot be performed based on a negative PET finding.[8)] A possible explanation for PET false negatives during initial staging is the presence of small lesions (< 0.5 cm or < 1 cm) and mature teratomas.[9)] On the other hand, the literature regarding the role of PET in staging seminomas is insufficient. Based on the above considerations, it was concluded that there is no clear basis for recommending PET for staging.

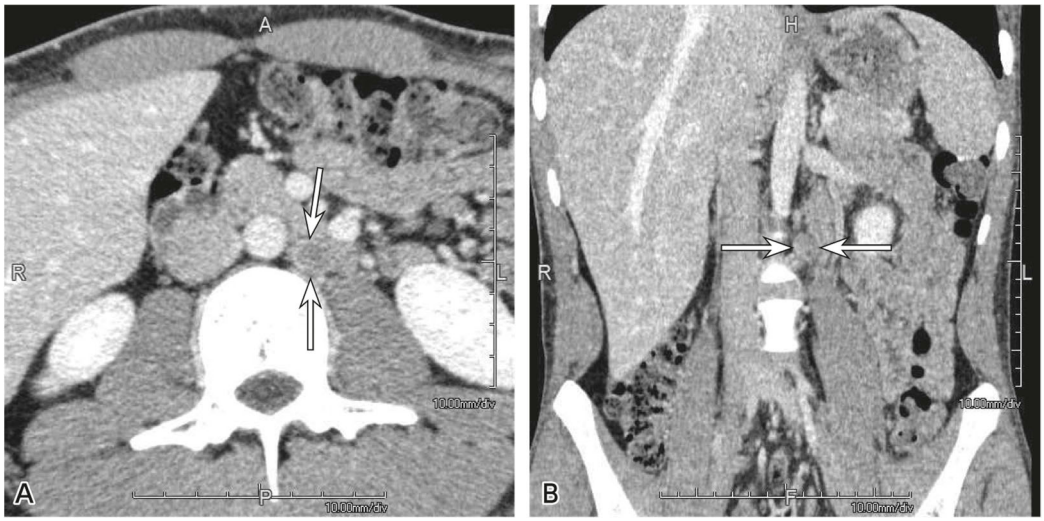

Figure. Patient who underwent high orchiectomy for a left testicular tumor

A: Contrast-enhanced CT, transverse image; B: Contrast-enhanced CT, coronal image
Enlarged paraaortic lymph node: 10 mm × 14 mm in the transverse image with craniocaudal length of 17 mm in the coronal image. Metastasis suspected (A, B →). Diagnosed as a stage IIA nonseminoma.

Search keywords and secondary sources used as references

PubMed was searched using the following keywords: testicular neoplasms, seminoma, nonseminoma, CT, and PET.

In addition, the following were referenced as secondary sources.

1) Japanese Urological Association, Ed.: 2015 Clinical Practice Guidelines for Testicular Tumors. KANEHARA & Co., 2015.
2) Yacoub JH et al: ACR Appropriateness Criteria®: staging of testicular malignancy. J Am Coll Radiol 13 (10), 1203-1209, 2016
3) Laguna MP et al: EAU guidelines on testicular cancer 2020. European Association of Urology, 2020

References

1) van Dijk MR et al: Survival of non-seminomatous germ cell cancer patients according to the IGCC classification: an update based on meta-analysis. Eur J Cancer 42: 820-826, 2006.
2) Hilton S et al: CT detection of retroperitoneal lymph node metastases in patients with clinical stage I testicular nonseminomatous germ cell cancer: assessment of size and distribution criteria. AJR Am J Roentgenol 169: 521-525, 1997
3) Hudolin T et al: Correlation between retroperitoneal lymph node size and presence of metastases in nonseminomatous germ cell tumors. Int J Surg Pathol 20: 15-18, 2012
4) Howard SA et al: Craniocaudal retroperitoneal node length as a risk factor for relapse from clinical stage I testicular germ cell tumor. AJR Am J Roentgenol 203: W415-420, 2014
5) Horan G et al: CT of the chest can hinder the management of seminoma of the testis: it detects irrelevant abnormalities. Br J Cancer 96: 882-885, 2007
6) de Wit M et al: [18F]-FDG-PET in clinical stage I/II non-seminomatous germ cell tumours: results of the German multicentretrial. Ann Oncol 19: 1619-1623, 2008
7) Lassen U et al: Whole-body FDG-PET in patients with stage I non-seminomatous germ cell tumours. Eur J Nucl Med Mol Imaging 30: 396-402, 2003
8) Huddart RA et al: ^{18}fluorodeoxyglucose positron emission tomography in the prediction of relapse in patients with high-risk, clinical stage I nonseminomatous germ cell tumors: preliminary report of MRC trial TE22: the NCRI Testis Tumour Clinical Study Group. J Clin Oncol 25: 3090-3095, 2007
9) De Santis M et al: The role of positron emission tomography in germ cell cancer. World J Urol 22: 41-46, 2004

BQ 76 Which imaging examinations are recommended for the posttreatment evaluation of a testicular tumor?

Statement

CT is recommended for evaluation after chemotherapy for a testicular tumor.

FDG-PET has a high negative predictive value in evaluating the viability of residual masses (particularly for masses ≥ 3 cm in size) after chemotherapy for seminomas and can therefore contribute to determining a treatment strategy. There is insufficient scientific evidence regarding the posttreatment evaluation of nonseminomas by FDG-PET, and it is therefore not recommended for this purpose.

Background

Recent advances in chemotherapy have led to striking improvement in the cure rate for advanced testicular tumors with metastasis. However, there is debate regarding the treatment strategy to adopt when residual masses are seen after chemotherapy. Residual masses are often only necrotic tissue and scar tissue containing no viable tumor cells, and retroperitoneal lymph node dissection (RPLND) is a highly invasive surgical procedure. Consequently, much is expected of residual mass evaluation by diagnostic imaging. This discussion provides an overview of the diagnostic imaging used for the post-chemotherapy evaluation of testicular tumors associated with metastasis, addressing seminomas and nonseminomas separately.

Explanation

Radical high orchiectomy is performed for testicular tumors without metastasis, with chemotherapy and radiation therapy added as necessary. To check for recurrence, periodic follow-up (surveillance) involving tumor marker measurement and abdominal CT is strongly recommended in multiple guidelines promulgated in other countries.

For metastatic seminomas, chemotherapy is performed in addition to high orchiectomy. It is also strongly recommended that tumor marker measurement and abdominal CT be performed for post-chemotherapy evaluation. Although residual masses are seen in 55% to 80% of patients after chemotherapy, many of these masses consist of necrotic or fibrous tissue. The conventional method used to assess the activity of residual masses has been to use a cutoff of 3 cm for the maximum diameter of a mass on CT. In reality, however, only 11-37% of residual masses ≥ 3 cm are found to be viable lesions.[1)]

FDG-PET has been reported to provide strong capability for evaluating the viability of residual masses after seminoma chemotherapy, particularly for masses ≥ 3 cm in size.[2-5)] Moreover, several international guidelines recommend FDG-PET for evaluating residual masses after seminoma chemotherapy. On the other hand, it has occasionally been reported that FDG-PET produces many false positives.[6-9)] In a systematic review published in 2014, pooled analysis results showed that the sensitivity, specificity, positive predictive value, and negative predictive value of FDG-PET were 78%, 86%, 58%, and 94%,

respectively.[10] The negative predictive values that have been reported for FDG-PET have been high, generally ≥ 90%.[1, 2, 4-7] Consequently, if a patient is negative on FDG-PET performed ≥ 6 weeks after chemotherapy, the likelihood of a viable tumor is considered low even if the diameter of a residual mass is ≥ 3 cm, and additional treatment may be avoided. The reported positive predictive values have varied widely depending on the report, ranging from 23% to 100%. In a study of 90 patients positive for residual masses on FDG-PET that was published in 2018, the positive predictive value was low, at 23%, and it was 22% for patients with masses ≥ 3 cm in diameter.[9] Caution is therefore required when aggressively performing additional treatment based only on a positive FDG-PET/CT finding. The most recent guidelines of the European Association of Urology (EAU) recommend follow-up by FDG-PET or CT if there is no enlargement of the mass.

In a prospective, multicenter study of 641 patients with nonseminomatous testicular tumors that was published in 2000, the proportion of patients with masses that consisted only of postoperative necrotic tissue increased as the diameter of the residual mass, as measured on post-chemotherapy CT, decreased and as the reduction rate increased.[11] However, 28% of the patients had a viable residual tumor (teratoma or carcinoma) if the diameter of the residual mass was ≤ 9 mm, and 20% had a viable residual tumor if the rate of diameter reduction was ≥ 85%. In addition, a 2003 report indicated that, when retroperitoneal lymph node dissection (RPLND) was performed in 87 patients with residual tumors ≤ 20 mm in diameter after treatment with bleomycin, etoposide, and cisplatin (BEP), viable tumors were seen in 33%.[12] It can therefore be concluded that, with nonseminomas, the likelihood of a viable residual mass is relatively high even if the diameter of the post-chemotherapy mass is small.

With regard to FDG-PET evaluation after chemotherapy for nonseminomas, a prospective, multicenter study in which the results for all of the patients were confirmed histologically was conducted in 2008. It found the sensitivity, specificity, positive predictive value, and negative predictive value of FDG-PET to be 70%, 48%, 59%, and 51%, respectively, and its diagnostic accuracy rate to be 56%. The diagnostic accuracy rate was 55% for CT and 56% for tumor marker measurement. Thus, the results indicated that the addition of FDG-PET to CT and tumor marker measurement does not provide additional information for postoperative tissue prediction.[13] Another study identified the problem of residual mature teratomas resulting in false negatives with FDG-PET,[14] and use of FDG-PET is not recommended in the guidelines from other countries.

Search keywords and secondary sources used as references

PubMed was searched using the following keywords, and further selections were made from the selected articles: testicular, testis, germ cell tumor, tumor, cancer, carcinoma, seminoma, nonseminoma, CT, and PET.

In addition, the following were referenced as secondary sources.

1) Laguna MP et al: EAU guidelines on testicular cancer 2020. European Association of Urology, 2020
2) Gilligan T et al: NCCN Guidelines®: testicular cancer ver 2. 2021. National Comprehensive Cancer Network, 2021

References

1) Bachner M et al: 2-^{18}fluoro-deoxy-D-glucose positron emission tomography (FDG-PET) for postchemotherapy seminoma residual lesions: a retrospective validation of the SEMPET trial. Ann Oncol 23: 59-64, 2012
2) De Santis M et al: Predictive impact of 2-^{18}fluoro-2-deoxy-D-glucose positron emission tomography for residual postchemotherapy masses in patients with bulky seminoma. J Clin Oncol 19: 3740-3744, 2001
3) Becherer A et al: FDG PET is superior to CT in the prediction of viable tumour in post-chemotherapy seminoma residuals. Eur J Radiol 54: 284-288, 2005
4) Ambrosini V et al: 18F-FDG PET/CT impact on testicular tumours clinical management. Eur J Nucl Med Mol Imaging 41: 668-673, 2014
5) De Santis M et al: 2-^{18}fluoro-deoxy-D-glucose positron emission tomography is a reliable predictor for viable tumor in postchemotherapy seminoma: an update of the prospective multicentric SEMPET trial. J Clin Oncol 22: 1034-1039, 2004
6) Hinz S et al: The role of positron emission tomography in the evaluation of residual masses after chemotherapy for advanced stage seminoma. J Urol 179: 936-940, 2008
7) Siekiera J et al: Can we rely on PET in the follow-up of advanced seminoma patients? Urol Int 88: 405-409, 2012
8) Decoene J et al: False-positive fluorodeoxyglucose positron emission tomography results after chemotherapy in patients with metastatic seminoma. Urol Oncol 33: 23.e15-23.e21, 2015
9) Cathomas R et al: Questioning the value of fluorodeoxyglucose positron emission tomography for residual lesions after chemo- therapy for metastatic seminoma: results of an International Global Germ Cell Cancer Group registry. J Clin Oncol 36: 3381-3387, 2018
10) Treglia G et al: Diagnostic performance of fluorine-18-fluorodeoxyglucose positron emission tomography in the postchemotherapy management of patients with seminoma: systematic review and meta-analysis. Biomed Res Int 2014: 852681, 2014
11) Steyerberg EW et al: Retroperitoneal metastases in testicular cancer: role of CT measurements of residual masses in decision making for resection after chemotherapy. Radiology 215: 437-444, 2000
12) Oldenburg J et al: Postchemotherapy retroperitoneal surgery remains necessary in patients with nonseminomatous testicular cancer and minimal residual tumor masses. J Clin Oncol 21: 3310-3317, 2003
13) Oechsle K et al: ［18F］Fluorodeoxyglucose positron emission tomography in non seminomatous germ cell tumors after chemotherapy: the German multicenter positron emission tomography study group. J Clin Oncol 26: 5930-5935, 2008
14) De Santis M et al: The role of positron emission tomography in germ cell cancer. World J Urol 22: 41-46, 2004

BQ 77 Which imaging examinations are recommended to diagnose adrenal adenomas?

Statement

Non-contrast CT and dynamic contrast-enhanced CT are strongly recommended.

Chemical shift MRI is more sensitive than non-contrast CT and is recommended.

Background

In recent years, with the development and widespread adoption of diagnostic imaging, mass lesions in the adrenals have frequently been detected by chance (incidentalomas) in imaging examinations performed for other purposes. Adrenal incidentalomas have been reported in 5% of CT examinations.[1, 2] Approximately 75% of adrenal incidentalomas are adrenal adenomas.[2] Diagnosing adrenal adenomas is therefore important for the differential diagnosis of adrenal masses. This discussion provides an overview regarding CT and chemical shift MRI, which are commonly used to diagnose adrenal adenomas.

Explanation

Two main approaches are taken to diagnosing adrenal adenomas by CT and MRI based on the presence or absence of lipids and the contrast enhancement pattern. Adenomas show lower attenuation than metastatic tumors on non-contrast CT due to the abundant presence of intracellular lipids. A meta-analysis showed that when a mean intratumoral CT number of < 10 HU was considered indicative of adenoma, sensitivity and specificity were 71% and 98%, respectively.[3] This diagnostic criterion was also adopted for the ACR Appropriateness Criteria® (secondary source 1). Using the mean CT number of < 10 HU as the diagnostic criterion enables approximately 70% of adenomas to be diagnosed with non-contrast CT.[3] In examinations of methods other than using the mean CT number, when CT numbers of all the pixels in a mass were analyzed using histograms, and masses in which ≥ 10% of the pixels had a CT number of < 0 HU or the 10th percentile of the CT numbers (mean CT number - [1.282 × standard deviation]) was < 0 HU were considered adenomas, sensitivity ranged from 84% to 91%.[4-6] If these methods can be used to diagnose adenomas by non-contrast CT, additional imaging examinations are unnecessary.[7]

Adrenal adenomas have the characteristics of medullary tumors, which have little fibrous compared with metastatic tumors, and the contrast-enhanced washout rate is high. The contrast-enhanced washout rate with the use of dynamic contrast-enhanced CT is quantitatively measured as follows: ① with pre-contrast CT: (early-phase CT number - late-phase CT number) / (early-phase CT number - pre-contrast CT number); and ② without pre-contrast CT: (early-phase CT number - late-phase CT number) / (early-phase CT number). Using images acquired 1 min (early phase) and 15 min after contrast injection (late phase), diagnostic performance with respect to masses that could not be diagnosed as adrenal adenomas (mean CT number of < 10 HU) by pre-contrast CT showed ① sensitivity and specificity of 86% and 92%, respectively,

when non-contrast CT was performed (washout rate > 60%) and ② sensitivity and specificity ranging from 77% to 82% and 89% to 92%, respectively, when pre-contrast CT was not performed (washout rate > 40%).[8, 9)]

For lipid detection, chemical shift MRI is more sensitive than CT and is particularly superior for detecting small quantities of lipids. The presence of lipids is suggested and adenoma can be diagnosed when the signal drop is seen in opposed-phase imaging compared with in-phase imaging.[10, 11)] For quantitative evaluation, the following methods are used to calculate the tumor signal intensity index and the tumor-to-spleen signal intensity ratio: ① tumor signal intensity index: tumor signal intensity on in phase - tumor signal intensity on opposed phase) / tumor signal intensity on in phase, and ② tumor-to-spleen signal intensity ratio: tumor-to-spleen signal intensity on opposed phase / tumor-to-spleen signal intensity on in phase. When the tumor signal intensity index is ≥ 16.5%, or the tumor-to-spleen signal intensity ratio is ≤ 71%, sensitivity and specificity range from 81% to 100% and 94% to 100%, respectively, enabling diagnosis.[1, 5, 12)] A meta-analysis found no difference in the diagnostic performance of qualitative and quantitative evaluations.[13)] When a cutoff of 20% was used for the tumor signal intensity index, sensitivity and specificity with respect to masses that could not be diagnosed as adrenal adenomas (mean CT number of > 10 HU) by non-contrast CT were 67% and 100%, respectively.[14)] Moreover, the diagnostic performance of chemical shift MRI was higher than that of CT histogram analysis.[15)] An investigation that compared the diagnostic performance of chemical shift MRI and dynamic contrast-enhanced CT in masses that could not be diagnosed as adrenal adenomas by non-contrast CT (mean CT number > 10 HU) found dynamic contrast-enhanced CT to be useful, with diagnostic accuracy of 88.1% (sensitivity, 91.7%; specificity, 74.8%) for dynamic contrast-enhanced CT and 73.6% (sensitivity, 67.1%; specificity, 88.7%) for chemical shift MRI.[16)] Consequently, although chemical shift MRI has diagnostic performance limitations in masses that cannot be diagnosed by non-contrast CT,[14, 17)] as is the case for non-contrast CT, it is recommended as a noninvasive examination with high specificity.

With all of the diagnostic methods that use the lipid detection and contrast enhancement patterns described above, there are false positives for neoplasms such as adrenocortical carcinoma, clear cell renal cell carcinoma, hepatocellular carcinoma, and pheochromocytoma.[18-21)] Attention is therefore also paid to clinical information such as past history, tumor size, and enlargement trends.

With regard to diffusion-weighted imaging, it has been reported that, in adrenal masses that are difficult to diagnose by chemical shift MRI, lesions with an apparent diffusion coefficient (ADC) of > 1.50 ± 10^{-3} mm^2/s are highly likely to be adenomas.[22)] However, the converse results, where ADC values of adenomas were lower than those of malignant tumors, have also been reported,[23)] as have results showing no significant difference between the ADC values of adenomas and metastatic tumors.[24)] Consequently, no conclusion has been reached in this regard.

Search keywords and secondary sources used as references

PubMed was searched using the following keywords, and further selections were made from the results: adrenal, adrenocortical, adenoma, mass, tumor, incidentaloma, pheochromocytoma, imaging, metastasis, computed tomography, magnetic resonance imaging, and positron emission tomography.

In addition, the following was referenced as a secondary source.

1) Choyke PL et al: ACR Appropriateness Criteria®: incidentally discovered adrenal mass. J Am Coll Radiol 3: 498-504, 2006

References

1) Boland GW et al: Incidental adrenal lesions: principles, techniques, and algorithms for imaging characterization. Radiology 249: 756-775, 2008
2) Song JH et al: The incidental adrenal mass on CT: prevalence of adrenal disease in 1,049 consecutive adrenal masses in patients with no known malignancy. AJR Am J Roentgenol 190: 1163-1168, 2008
3) Boland GW et al: Characterization of adrenal masses using unenhanced CT: an analysis of the CT literature. AJR Am J Roentgenol 171: 201-204, 1998
4) Ho LM et al: Lipid-poor adenomas on unenhanced CT: does histogram analysis increase sensitivity compared with a mean attenuation threshold? AJR Am J Roentgenol 191: 234-238, 2008
5) Halefoglu AM et al: Differentiation of adrenal adenomas from nonadenomas using CT histogram analysis method: a prospective study. Eur J Radiol 73: 643-651, 2010
6) Rocha TO et al: Histogram analysis of adrenal lesions with a single measurement for 10th percentile: feasibility and incremental value for diagnosing adenomas. AJR Am J Roentgenol 211: 1227-1233, 2018
7) Garrett RW et al: Adrenal incidentalomas: clinical controversies and modified recommendations. AJR Am J Roentgenol 206: 1170-1178, 2016
8) Caoili E M et al: Adrenal masses: characterization with combined unenhanced and delayed enhanced CT. Radiology 222: 629-633, 2002
9) Marty M et al: Diagnostic accuracy of computed tomography to identify adenomas among adrenal incidentalomas in an endocrinological population. Eur J Endocrinol 178: 439-446, 2018
10) Korobkin M et al: Characterization of adrenal masses with chemical shift and gadolinium-enhanced MR imaging. Radiology 197: 411-418, 1995
11) Mitchell DG et al: Benign adrenocortical masses: diagnosis with chemical shift MR imaging. Radiology 185: 345-351, 1992
12) Fujiyoshi F et al: Characterization of adrenal tumors by chemical shift fast low-angle shot MR imaging: comparison of four methods of quantitative evaluation. AJR Am J Roentgenol 180: 1649-1657, 2003
13) Platzek I et al: Chemical shift imaging for evaluation of adrenal masses: a systematic review and meta-analysis. Eur Radiol 29: 806-817, 2019
14) Haider MA et al: Chemical shift MR imaging of hyperattenuating (> 10 HU) adrenal masses: does it still have a role? Radiology 231: 711-716, 2004
15) Jhaveri KS et al: Comparison of CT histogram analysis and chemical shift MRI in the characterization of indeterminate adrenal nodules. AJR Am J Roentgenol 187: 1303-1308, 2006
16) Koo H J et al: The value of 15-minute delayed contrast-enhanced CT to differentiate hyperattenuating adrenal masses compared with chemical shift MR imaging. Eur Radiol 24: 1410-1420, 2014
17) Park BK et al: Comparison of delayed enhanced CT and chemical shift MR for evaluating hyperattenuating incidental adrenal masses. Radiology 243: 760-765, 2007
18) Patel J et al: Can established CT attenuation and washout criteria for adrenal adenoma accurately exclude pheochromocytoma? AJR Am J Roentgenol 201: 122-127, 2013
19) Choi YA et al: Evaluation of adrenal metastases from renal cell carcinoma and hepatocellular carcinoma: use of delayed contrast-enhanced CT. Radiology 266: 514-520, 2013
20) Heye S et al: Adrenocortical carcinoma with fat inclusion: case report. Abdom Imaging 30: 641-643, 2005
21) Moosavi B et al: Intracellular lipid in clear cell renal cell carcinoma tumor thrombus and metastases detected by chemical shift (in and opposed phase) MRI: radiologic-pathologic correlation. Acta Radiol 57: 241-248, 2016
22) Sandrasegaran K et al: Characterization of adrenal masses with diffusion-weighted imaging. AJR Am J Roentgenol 197: 132-138, 2011
23) Song J1 et al: Utility of chemical shift and diffusion-weighted imaging in characterization of hyperattenuating adrenal lesions at 3.0T. Eur J Radiol 81: 2137-2143, 2012

24) Tsushima Y et al: Diagnostic utility of diffusion-weighted MR imaging and apparent diffusion coefficient value for the diagnosis of adrenal tumors. J Magn Reson Imaging 29: 112-117, 2009